Acta Astronautica 144 (2018) 225–243

Contents lists available at ScienceDirect

Acta Astronautica

journal homepage: www.elsevier.com/locate/actaastro

Assessment of active methods for removal of LEO debris

Houman Hakima [a], M. Reza Emami [a,b,*]

[a] Institute for Aerospace Studies, University of Toronto, 4925 Dufferin Street, Toronto, Ontario M3H 5T6, Canada
[b] Onboard Space Systems, Space Technology Division, Luleå University of Technology, Kiruna 98128, Sweden

A B S T R A C T

This paper investigates the applicability of five active methods for removal of large low Earth orbit debris. The removal methods, namely net, laser, electrodynamic tether, ion beam shepherd, and robotic arm, are selected based on a set of high-level space mission constraints. Mission level criteria are then utilized to assess the performance of each redirection method in light of the results obtained from a Monte Carlo simulation. The simulation provides an insight into the removal time, performance robustness, and propellant mass criteria for the targeted debris range. The remaining attributes are quantified based on the models provided in the literature, which take into account several important parameters pertaining to each removal method. The means of assigning attributes to each assessment criterion is discussed in detail. A systematic comparison is performed using two different assessment schemes: Analytical Hierarchy Process and utility-based approach. A third assessment technique, namely the potential-loss analysis, is utilized to highlight the effect of risks in each removal methods.

1. Introduction

Following 60 years of space exploration and utilization, we have ended up with tens of thousands of pieces of man-made debris around our planet. Despite the increasing number of satellite launches, only a small portion of them has been deorbited, i.e., moved to a lower orbit where atmospheric drag would eventually decay the satellite's orbit to its burn-up fate. As a result, a great majority of in-orbit satellites, nearly 90%, are decommissioned and their missions have been terminated [1].

Currently, the Intentional Telecommunication Union (ITU) requires satellites in the geostationary orbit (GEO) to move to a *graveyard* orbit at the end of their mission [2]. Similarly, for the low Earth orbit (LEO) satellites, the Inter-Agency Space Debris Coordination Committee (IADC) has recommended that LEO satellites remove themselves within 25 years, after the termination of their mission [3]. As a result, many small and large satellite institutions have accordingly begun developing end-of-life debris mitigation strategies.

Despite the above-mentioned regulations for debris mitigation, computer simulations have shown that, unless controlled by some external mechanisms, the existing orbital debris population is self-propagating and their density will continue to increase through random debris inter-collisions [4]. Such cascading effect is known as "Kessler Syndrome" [5], which can eventually render some orbits impractical for future space missions. Fig. 1 shows a projected growth of debris in LEO with and without mitigation, starting in the year 2010. The trend clearly suggests that space activity is placing debris in orbit in a faster pace than the natural effects of atmospheric drag can remove it. Therefore, given the increasing trend of space activities, the only solution to control debris self-propagation seems to be their removal from orbit actively.

A widely accepted classification of LEO debris based on the size is presented in Table 1. Small pieces (<1 cm) are numerous and difficult to detect, but shielding against them is straightforward, albeit somewhat expensive. Medium objects (1–10 cm) have a large population, which makes it problematic to track all of them. They are too numerous to avoid, and shielding against them is very difficult and expensive. Finally, there are large objects (>10 cm) that are routinely tracked, and their numbers are small enough that operational spacecraft can maneuver to avoid them.

The objective of this paper is to systematically examine and compare the viability of the active methods for removing large LEO debris. The reason for targeting large debris is that they pose serious threat to the stability of the LEO debris environment. Aside from in-orbit explosions, the collision between large debris objects and their fragmentations are the main sources of smaller debris. Computer simulations have shown that in order to sustain the stability of LEO debris environment, it is necessary to remove at least five large debris per year [8–11]. The most recent status of the Earth-bound space debris is presented in Fig. 2. The figure shows the number of debris object larger than 10 cm, which are trackable by the United States Space Surveillance Network (SSN).

The rationale for focusing on low Earth orbit in this study is that, as shown in Fig. 2, out of roughly 17,500 cataloged debris (as of Oct 1,

* Corresponding author. Institute for Aerospace Studies, University of Toronto, 4925 Dufferin Street, Toronto, Ontario M3H 5T6, Canada.
E-mail addresses: houman.hakima@mail.utoronto.ca (H. Hakima), emami@utias.utoronto.ca, reza.emami@ltu.se (M.R. Emami).

https://doi.org/10.1016/j.actaastro.2017.12.036
Received 1 November 2017; Accepted 24 December 2017
Available online 4 January 2018

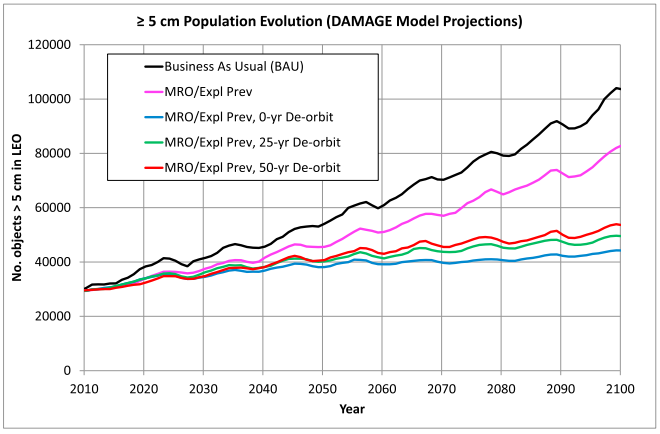

Fig. 1. Debris growth with various mitigation approaches [6]. MRO/Expl Prev: mission related objects (MRO) and explosion prevention.

Table 1
Space debris in LEO, according to the generally accepted categorization [7].

	Categories		
	Small	Medium	Large
Size (cm)	<1	1–10	>10
Risk	Damage can be shielded	Partial/total destruction	Complete destruction
Detection	Not tracked; statistically addressed	Partially tracked	Tracked
Estimated No.	> 100 million	~ 500,000	> 21,000
Mass Fraction	–	5%	95%

2017), more than 12,500 reside in LEO. Several studies (e.g., Refs. [4,10,13,14]) have predicted that if no large debris is removed from LEO, the debris population will have a rapid increase in the next couple of decades, due to the possible inter-collisions. This is especially relevant to the sun-synchronous orbits around 1000 km where the probability of catastrophic collisions is much higher than that of other regions [14]; whereas the non-mitigation scenarios predict a moderate population growth in the medium Earth orbit (MEO) and the geosynchronous orbit (GSO). Further, the number of operational satellites in LEO is considerably higher than those in MEO and GEO combined. Indeed, LEO can be considered as the most densely populated regime (using the spherical shell densities) making debris removal in LEO of higher priority. Nevertheless, It is worth mentioning that since 95% of insured satellite systems reside in GEO (roughly $18.3 billion) [15,16], the economic impact of a GEO satellite getting struck by debris should not be undermined.

This paper is organized as follows: Section 2 outlines the major mission constraints. Section 3 outlines the assessment criteria used in this study. Section 4 describes the removal methods applicable to this study. Section 5 explains the removal scenarios. Section 6 presents the preliminary evaluation of the assessment attributes. Section 7 describes the selected assessment approaches. Section 8 discusses the performance of each removal method with regard to the various criteria and assessment approaches considering the quantified result. Lastly, Section 9 presents the concluding remarks and suggestions for future works.

2. Problem formulation

To provide a valid baseline for the comparative analysis, the removal methods considered in this study are constrained with respect to the following factors:

- Debris size: Removal methods that are potentially capable of removing medium and large debris objects are considered in this study.
- Removal agent: Even though several *self-removal* methods have been considered in the literature related to active debris removal (ADR), this study focuses on methods that employ external agents for debris removal. As a result, the end-of-life disposal techniques will not be considered in this study.
- Non-destructive methods: Several of the proposed ADR methods in the literature are either potentially destructive (e.g., kinetic impactors), or explicitly destructive (e.g., nuclear bombs). These methods can cause further fragmentation of the orbital debris, and adversely affect the debris environment. In this assessment, methods that are naturally non-destructive will be considered.
- System mass and volume: The maximum mass and volume for the system is limited to the payload specification of an Atlas V 552 launch vehicle that is capable of transferring 18,850 kg to LEO and 8900 kg to geosynchronous transfer orbit (GTO) [17]. The stowed system volume should be less than a payload envelope of approximately 13 m in height and 5 m in width [17].

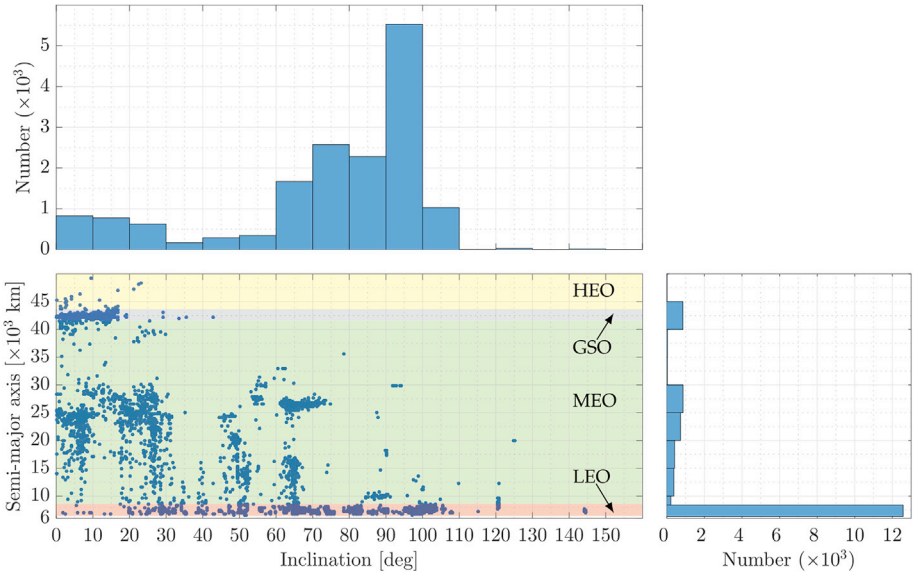

Fig. 2. Distribution of the tracked debris objects around Earth, as of Oct. 1, 2017 [12]. HEO: high Earth orbit.

- Technology readiness level (TRL): The key components of the removal methods must have a TRL of at least 3, i.e., their critical functions have been analytically and experimentally investigated. The restriction on the TRL ensures that the removal method has been sufficiently researched, and consequently the attributes can be readily assigned to the assessment criteria [18].

Based on the above-mentioned constraints, five ADR methods are considered in this paper, which are described in detail in Section 4.

2.1. Simulation description

The reference database that is utilized in this study is the Satellite Catalog, SATCAT. The catalog is a comprehensive list of all man-made space objects that have ever flown into space. Aside from listing the names and NORAD numbers of the objects, SATCAT gives information regarding the orbital parameters (period, inclination, and apogee and perigee heights), as well as the current operational status of the listed objects (see Table 2) and their radar cross sections, RCS.

Before using the SATCAT, a number of pre-filters had to be applied to the catalog to determine the candidate debris population. First, the operational satellites had to be removed from the study. As such, *active* objects (i.e., "+", "P", "B", "S", or "X" [19]) and decayed objects (i.e., "D") were rejected. Second, the study only considers objects that are within LEO. As such, those with semi-major axes larger than 8378 km were also rejected. Third, a large number of objects that are listed in the SATCAT are debris fragment that are remnants of on-orbit explosions and collisions. These fragments are generally identified by letter "DEB" postfixed to their names. For example, the Thor-Ablestar rocket body (NORAD 118, launched in 1961) has 28 trackable fragments in orbit. Since the objects of interest in this study are the large ones, any object with the suffix "DEB" in its name and with an RCS smaller than 0.1 m^2 (i.e., small) was rejected. Forth, since ADR missions are costly and complex operations, the ADR priority must given to the heavier and larger objects, typically those with masses over 1 ton. As such, the lower threshold of mass was set to 1000 kg in this study. Fifth and last, it was determined that the debris' orbit inclination had to be confined to the range 70°–100°, for two reasons. On the one hand, inclination change maneuvers are very costly in terms of delta-v (and propellant). Hence, if the remover spacecraft is required to travel between orbits with considerable inclination difference, the amount of required propellant (and time) to perform the maneuver would make the study unrealistic, and the mission impossible. On the other, As was shown in Fig. 2, the vast majority of debris objects in LEO (more than 9000) are in the 70°–100° inclination range, which includes polar and near polar orbits.

After applying the aforementioned prefilters to the database, 650 debris objects (as of Oct 1, 2017) were left that qualified as potential target debris for this study. Fig. 3 shows the histograms of the semi-major axis (a), inclination (i), eccentricity (e), and mass of the candidate debris population. A Monte Carlo simulation has been created which runs for a total of 1000 iterations. At each iteration, the simulation randomly selects five objects from the candidate debris population, and uses their orbital parameters as well as their mass values (obtained mainly from ESA's DISCOS database [20]) to compute the orbital maneuver times and the amount of required propellant by each removal method.

Table 2
SATCAT operational status [19].

Operational Status	Description	Operational Status	Description
+	Operational	S	Spare
–	Nonoperational	X	Extended mission
P	Partially operational	D	Decayed
B	Backup/standby	?	Unknown

As shown in Fig. 3(c), the great majority of debris objects in LEO tend to have very small orbit eccentricities. As such, this study assumes that debris objects are in circular orbits (i.e., $e = 0$). Lastly, since the position of an object in its orbit continuously changes with time, the simulation randomly assigns a value to the angular distance between the remover spacecraft and the target debris, $\Delta\theta$, in the range $-\pi$ to π. Similarly, due to the constant drift of right ascension of the ascending node (RAAN), the simulation randomly assigns a value between $-\pi$ to π to the RAAN difference between the remover's and debris' orbits, $\Delta\Omega$.

3. Assessment criteria

The assessment criteria for this study represent a combination of standard space mission parameters and those specific to debris removal missions. The criteria are defined in Table 3, and detailed in subsequent sections.

3.1. Removal time

The removal time refers to the total time it takes each removal method to successfully deorbit all 5 debris selected by the Monte Carlo simulation. It is consisted of two types of maneuvers, namely the orbital maneuver and proximity maneuver, each detailed in the following sections. The total removal time, Δt_{rmv}, is then obtained by summing the time each of the maneuvers requires, i.e., $\Delta t_{\text{rmv}} = \Delta t_{\text{orb}} + \Delta t_{\text{prx}}$ where Δt_{orb} and Δt_{prx} denote the orbital maneuver time and proximity maneuver time, respectively.

3.1.1. Orbital maneuvers

Orbital maneuvers are performed by the remover spacecraft in order to reach the target debris' orbit, as well as to move the debris from its initial orbit to the deorbit altitude of 150 km. This work considers four types of orbital maneuvers, namely, the semi-major axis change, inclination change, right ascension of ascending node (RAAN) correction, and orbit phasing. The magnitude of required delta-v, Δv_{sma}, and the required time, Δt_{sma}, to change the semi-major axis from a_1 to a_2, are obtained from the following:

$$\Delta v_{\text{sma}} = \left| \sqrt{\frac{\mu_\oplus}{a_1}} - \sqrt{\frac{\mu_\oplus}{a_2}} \right| \tag{1a}$$

$$\Delta t_{\text{sma}} = \frac{\Delta v_{\text{sma}} m_{\text{rem}}}{F_{\text{th}}} \tag{1b}$$

where $\mu_\oplus$ is the standard gravitational parameter of Earth, m_{rem} is the mass of the remover spacecraft, and F_{th} is the thrust force supplied by the propulsion system.

Note that Δv_{sma} calculation in Eq. (1a) is based on the low-thrust propulsion and not an impulsive maneuver, i.e., Hohmann transfer. Therefore, Δv_{sma} is notably larger than Hohmann's Δv. Equations (1a) and (1b) are also used to calculate the required delta-v and time to perform the deorbitation (denoted by Δv_{do} and Δt_{do}, respectively), with $a_2 = R_\oplus + 150$ km where $R_\oplus = 6,378$ km denotes the Earth radius. Also, in Eq. (1b), m_{rem} should be replaced with system's mass, m_{sys}, where $m_{\text{sys}} = m_{\text{deb}} + m_{\text{rem}}$ in contact methods (the remover spacecraft "carries" the debris), and $m_{\text{sys}} = m_{\text{rem}}$ in contactless removal methods since the remover spacecraft changes the debris orbit without any physical contact.

The change of inclination and RAAN correction maneuvers are necessary to make the remover spacecraft and the target debris co-planar. The amount of required delta-v, Δv_{inc}, and the time it takes to change the inclination, Δt_{inc}, are obtained from the following [21]:

$$\Delta v_{\text{inc}} = \sqrt{\frac{\mu_\oplus}{a}} \sqrt{2 - 2\cos\left(\frac{\pi}{2}\Delta i\right)} \tag{2a}$$

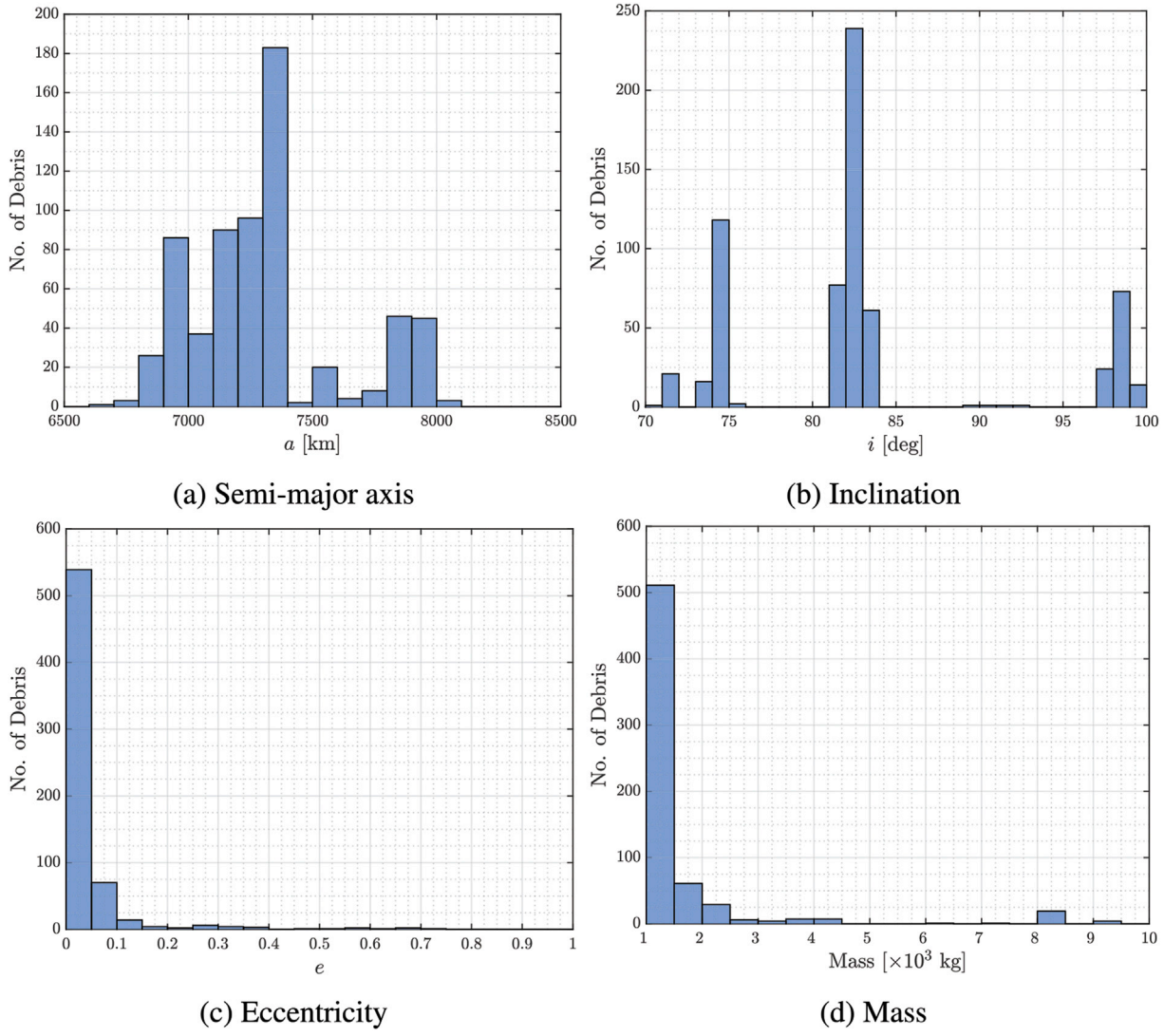

Fig. 3. Histograms of the candidate debris's orbital parameters and masses; Population size = 650.

$$\Delta t_{\text{inc}} = \frac{\Delta v_{\text{inc}} m_{\text{rem}}}{F_{\text{th}}} \tag{2b}$$

where Δi is the desired change in inclination. The amount of required delta-v, Δv_{raan}, and the time it takes to correct RAAN, Δt_{raan}, are obtained from the following [21]:

$$\Delta v_{\text{raan}} = \frac{\pi}{2}\sqrt{\frac{\mu_{\oplus}}{a}}\left|\Delta\Omega\right|\sin i \tag{3a}$$

$$\Delta t_{\text{raan}} = \frac{\Delta v_{\text{raan}} m_{\text{rem}}}{F_{\text{th}}} \tag{3b}$$

As seen in Eqs (2a) and (3a), a larger a leads to smaller Δv_{inc} and Δv_{raan}. As such, the inclination/RAAN change maneuvers are performed prior to the semi-major axis change maneuver if the remover spacecraft's current orbit is larger than that of the target debris' orbit, and vice versa.

Lastly, the orbit phasing is required to bring the angular distance (denoted by $\Delta\theta$) between the remover spacecraft and the target debris to zero when both objects are in the same orbit. The general approach for performing the orbit phasing is to transfer the remover spacecraft to a lower (when $\Delta\theta > 0$) or a higher (when $\Delta\theta < 0$) nearby orbit, then coast in this new intermediate orbit, and finally return to the original orbit. By adjusting the thrusting time, the phasing maneuver duration can be adjusted. The relation between the total thrusting time, Δt_{th}, and the total phasing time, Δt_{ph}, is described by the following quadratic equation [22]:

$$\frac{1}{2}\Delta t_{\text{th}}^2 - \Delta t_{\text{th}}\Delta t_{\text{ph}} + \frac{2}{3}\frac{m_{\text{rem}} a_0 \Delta\theta}{F_{\text{th}}} = 0 \tag{4}$$

where a_0 is the semi-major axis of the original orbit. In Eq. (4), phasing can be accomplished with different choices of thrusting time; a smaller Δt_{th} yields to a larger Δt_{ph}, while always $\Delta t_{\text{th}} \leq \Delta t_{\text{ph}}$. A limiting case is when $\Delta t_{\text{th}} = \Delta t_{\text{ph}}$, i.e., when the remover spacecraft continuously thrusts during the orbit phasing and hence coasting is avoided all together, resulting in minimum Δt_{ph}. Fig. 4 shows two hypothetical scenarios in which a 1-ton remover spacecraft follows a debris in a 1000 km orbit (i.e., $a_0 = 7,378$ km), with an initial angular distance of $\Delta\theta = \pi/4$ from the debris, assuming $F_{\text{th}} = 0.4$ N. Fig. 4(a) corresponds to the minimum phasing time case, but in Fig. 4(b), it is assumed that the remover thrusts for one-third of the phasing maneuver, i.e., $\Delta t_{\text{th}} = 1/3{\cdot}\Delta t_{\text{ph}}$. The continuous-thrust strategy during orbit phasing minimizes the maneuver time at the expense of producing a larger delta-v and hence using more propellant.

The total orbital maneuver time, Δt_{orb}, is then calculated from the following:

$$\Delta t_{\text{orb}} = \Delta t_{\text{sma}} + \Delta t_{\text{do}} + \Delta t_{\text{inc}} + \Delta t_{\text{raan}} + \Delta t_{\text{ph}} \tag{5}$$

Table 3
Assessment criteria (adopted from Ref. [18]).

ID	Criteria	Description	Metric
AC-1	Removal time	The total time it takes the removal method to successfully deorbit 5 debris. A smaller removal time is preferred.	Δt_{rmv} (days)
AC-2	Performance robustness	The ability of the system to resist a change due to variations in debris parameters such as mass and orbit altitude. A greater robustness is preferred.	Coefficient of variation of time, c_t
AC-3	Controlled re-entry	The ability of the system to re-enter the debris into the Earth's atmosphere over an unpopulated area. In accordance with the IADC guidelines, controlled re-entries are preferred.	$\mathscr{X}_{\text{CR}}$ (0 or 1)
AC-4	Propellant mass	The total mass of propellant required to accomplish the removal mission for each specific removal method. Lower propellant mass if preferred	m_{prp} (kg)
AC-5	Total mission cost	The total cost of the removal mission, from the development of the method to completion of the mission. Lower total mission cost is preferred.	Total mission cost, $\mathscr{T}$ (USD)
AC-6	Average Required Power	The average electrical power required for operation of the removal method. Lower power is preferred.	P (W)
AC-7	Technology Readiness and Risk	The technological readiness and risk assessment (TRRA) value will consider the TRL, the advancement degree of difficulty (AD^2), and the technology need value (TNV) for the removal method. A lower integrated technological risk is preferred.	Integrated technology risk matrix
AC-8	Mission Risk	Any risk that may jeopardize the implementation or success of the mission. A lower risk is preferred.	Risk assessment matrix

3.1.2. Proximity maneuver

Proximity maneuver is performed when the remover spacecraft is in the vicinity of the target debris, and is typically consisted of three operations: attitude synchronization, capturing, detumbling, and the attachment of the thruster deorbiting kit (TDK) to the target debris. Depending on the removal method, the remover spacecraft may have to perform a combination of these four maneuvers.

During the synchronization operation, the remover spacecraft approaches the target debris in a way that the relative velocity between the end-effector on the remover spacecraft and the target grapple point is zero [23]. The capturing refers to the operation by which the remover spacecraft makes physical contact and grasps the debris from the grapple point. The detumbling operation refers to the passivation (stabilization) of a free-floating tumbling debris [23] using remover spacecraft's on-board attitude actuators, resulting in zero debris' inertial attitude rates. Lastly, TDK attachment refers to installation of the TDK module to the host debris, which is described in Section 4.

The detailed calculation of the time and consumed propellant mass during the proximity maneuver (Δt_{prx} and m_{prx}) is beyond the scope of this paper, and depends on the control techniques utilized during each operation. Moreover, considering that the orbital maneuvers are achieved by low-thrust propulsion systems, Δt_{orb} is expected to be much larger than Δt_{prx}. However, in order to distinguish between the contact and contactless methods and to account for the inherent complexity of the proximity maneuvers, the proximity time and consumed propellant will be included in the study.

The required delta-v to perform each proximity maneuver (i.e., attitude synchronization, capturing, detumbling, and TDK attachment) is obtained by adding 5% of the required delta-v to perform all other maneuvers: $\Delta v_{\text{prx}} = 0.5n{\cdot}\Delta v_{\text{orb}}$, where n is the number of required proximity operations. For instance, if a method requires all four operations, then $\Delta v_{\text{prx}} = 0.2{\cdot}\Delta v_{\text{orb}}$. A discussion of the types of maneuvers that each removal method requires is presented in Section 5.

3.2. Performance robustness

Using the average removal time, Δt_{rmv}, and standard deviation of removal time, $\sigma_{\Delta t_{\text{rmv}}}$, the performance robustness for the target population of debris can be assessed using the coefficient of variation c_t, calculated as follows:

$$c_t = \frac{\sigma_{\Delta t_{\text{rmv}}}}{\Delta t_{\text{rmv}}} \tag{6}$$

Clearly, the lower the value of c_t for a removal method, the higher the performance robustness of the method will be. Thus, performance robustness has an inverse relationship with the coefficient of variation (performance robustness $\propto 1/c_t$.)

3.3. Controlled Re-entry

Controlled reentry refers to the ability of a method to control the time

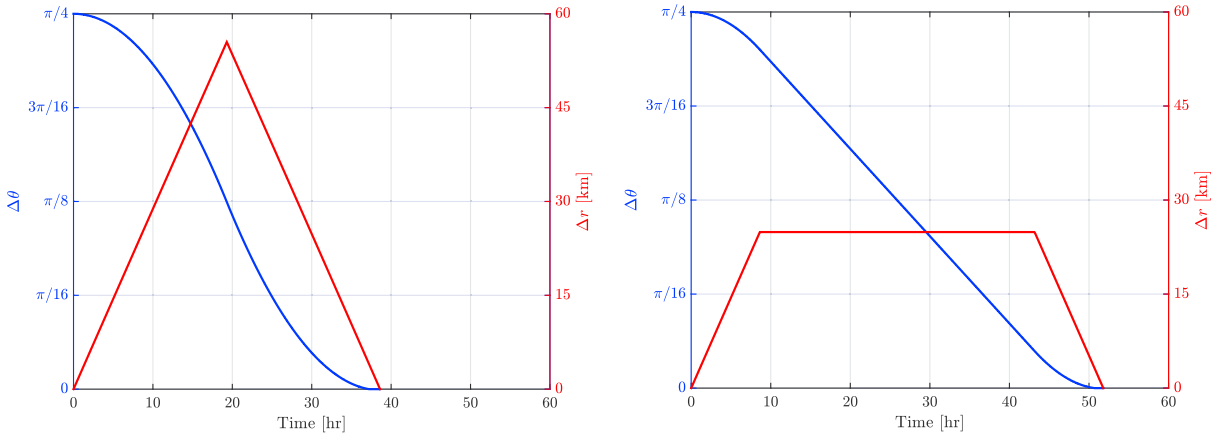

(a) $\Delta t_{\text{th}} = \Delta t_{\text{ph}}$ (i.e., no coasting). (b) $\Delta t_{\text{th}} = 1/3 \cdot \Delta t_{\text{ph}}$.

Fig. 4. Sample phasing maneuvers (Δr denotes the difference between orbital radii).

of reentry of the debris into the Earth's atmosphere, and to impact the debris in a confined, designated, unpopulated zone [24] such as the South Pacific Ocean Uninhabited Area (SPOUA). Since the removal methods in this study are assumed to be equipped only with low-thrust propulsion system, they cannot reenter the debris in a controlled manner. (Low thrust propulsion systems cannot provide the large acceleration that is required.) Further, the methods are considered to deorbit more than one debris, and hence they cannot directly take the debris to SPOUA. Instead, the spacecraft only transfers the debris to the deorbit altitude, and from there, some other methods have to be utilized to reenter the debris and crash-land it into SPOUA. In this study, the means for controlled reentry are the impulsive *thruster deorbiting kits (TDK)*. The spacecraft in contact methods are assumed to be capable of installing TDK modules to the target debris once they have reached the deorbit altitude of 150 km. The controlled reentry criteria is represented by a binary variable, $\mathscr{X}_{\mathrm{CR}}$, that is equal to 1 if the method is compliant with the controlled reentry requirement, and 0 otherwise. It follows that:

$$\mathscr{X}_{\mathrm{CR}} = \begin{cases} 1, & \text{for contact methods} \\ 0, & \text{for contactless methods} \end{cases} \tag{7}$$

3.4. Propellant mass

The propellant mass, m_{prp}, required to perform each of the orbital maneuvers (semi-major axis change, inclination change, and orbit phasing) can be estimated from the following:

$$\frac{m_{\mathrm{prp}}}{m'_{\mathrm{rem}}} = \exp\left(\frac{\Delta v}{I_{\mathrm{sp}} g}\right) - 1 \tag{8}$$

where m'_{rem} denotes the mass of the remover spacecraft after the maneuver is performed.

3.5. Mission cost

The mission cost is primarily comprised of four elements: a) cost of development of the removal method, b) launch cost, c) ground station retrofitting cost, and d) operations cost. The development cost, also referred to as the system cost, can be estimated using NASA's single Cost Estimate Relationship (CER) QuickCost regression model. The model is a statistically-based, cost predicting algorithm derived from historical data [25]. It utilizes relationships between key mission parameters to estimate the cost of the mission from Phase B through Phase D (NASA program phases), and does not include the cost of launch. The governing equation for the QuickCost regression model is as follows [26]:

$$\begin{aligned} \mathscr{D} = {} & 2.829 \times \mathrm{Dry\ Mass}^{0.457} \times \mathrm{Power}^{0.157} \times 2.718^{(0.171 \times \mathrm{Data\%})} \\ & \times 2.718^{0.00209 \times \mathrm{Life}} \times 2.718^{1.52 \times \mathrm{New}} \times 2.718^{0.258 \times \mathrm{Planetary}} \\ & \times \frac{1}{2.718^{0.00145 \times (\mathit{Year} - 1960)}} \times 2.718^{0.467 \times \mathrm{Instr\ Comp\%}} \times \frac{1}{2.718^{0.237 \times \mathrm{Team}}} \end{aligned} \tag{9}$$

where $\mathscr{D}$ is the total development cost in 2010 dollars. The remaining parameters of Eq. (9) are listed and described in Table 4. To convert the system cost to 2020 dollars, a conversion rate of 1.2179 is used. As a rough rule of thumb, one can add 2% to include Phase A costs, 9% to include the cost of retrofitting existing ground station, and 5% to include the cost of each year of mission operations and data analysis [26]. Another cost that needs to be taken into account is the launch cost, $\mathscr{L}$, which may be approximated using the following:

$$\mathscr{L} = m_{\mathrm{rem}} \cdot 20,000\ \$/\mathrm{kg} \tag{10}$$

where it has been assumed that the approximate cost of launching and placing a spacecraft to LEO using a heavy launch vehicle such as Atlas V is $\$20,000$ per kilogram of the spacecraft [27]. Putting all the costs together, the total mission cost, $\mathscr{T}$, can be obtained from the following:

Table 4
Parameters of CER QuickCost model (Eq. (9)) and their descriptions [26].

Parameter	Description
Dry Mass	Dry mass of spacecraft bus and instruments in kg
Power	LEO equivalent beginning of life power in watts
Data%	Data rate percentile relative to the state-of-the-art at authority to proceed (ATP): 0.5 for median data rate missions, < 0.5 for lower data rates, > 0.5 for higher data rates
Life	Advertised design life (in months), excluding extended operations
New	Percent new: 0.2–0.3 = Simple Mod, 0.3–0.7 = Extensive Mod, 0.7–1.0 = New, >1.0 for New Technology
Planetary	0 for earth orbital and 1 for planetary
Year	Date of authorization to proceed in 4 digit calendar year
InstrComp %	Instrument complexity percentile (fraction), relative to "average" instrument complexity: 0.5 for median complexity, <0.5 for lower complexity, and >0.5 for higher complexity
Team	Team experience: 1 = unfamiliar, 2 = mixed, and 3 = normal, and 4 = extensive

$$\mathscr{T} = 1.16\mathscr{D} + \mathscr{L} \tag{11}$$

3.6. Technology readiness and risk assessment

To understand the current maturity of the critical technologies for each removal method, and to quantify the potential risk of not meeting the expectations during the research and development (R&D) process, the integrated technology readiness and risk assessment (TRRA) is used [28]. The integrated TRRA decomposes each debris removal concept into functional areas corresponding to three key technologies, and then determines the three key R&D metrics for each technology. The three metrics are a) technology readiness level (TRL); b) advancement degree of difficulty (AD^2); and c) technology need value (TNV) [29]. These metrics are briefly introduced in the following section.

3.6.1. Technology readiness level

The technology readiness level (TRL), developed by NASA, represents a standardized scale for assessment of the maturity level of a particular technology. Each project is evaluated against the parameters for each technology level, followed by assigning a TRL rating based on the project progress [30]. There are nine technology readiness levels, as described in Table 16 in Appendix A. In this study, delta-TRL (ΔTRL) will be used to measure the level of maturity relative to a particular goal in a planned R&D program. It is simply the difference in TRLs between the current level of maturity of a particular technology and the desired level of maturity by a particular point in time in the future [29]. The desired TRL for the removal methods in this assessment is TRL 6, meaning the system model or prototype demonstrated in a relevant environment, such that the removal method will become ready for demonstration in space environment at the next level. Note that the *desired* TRL (of equal to 6) differs from the minimum required TRL for each removal method, which is equal to 3 (Section 2).

3.6.2. Advancement degree of difficulty

The advancement degree of difficulty (AD^2) is a systematic way of dealing with the uncertainty, i.e., probability of success and/or failure, in the planned technology development effort [31]. It is a predictive description of what is required to move a system, subsystem or component from one TRL to the next. It provides nine levels of risk, from 0% to 100%, as defined in Table 17 in Appendix A.

3.6.3. Technology need value

The technology need value (TNV) is a weighting factor based on the assessed importance of a particular technology development [28]. The technologies involved in debris removal methods are either critical to the functionality of the system, or beneficial to the success of the methods. In essence, TNV is the tool utilized for quantifying the significance of the technology to the removal method. Table 18 in Appendix A summarizes

the five TNV values used in the TRRA.

3.6.4. Integrated technology risk matrix

To aggregate the three key R&D metrics explained in Sections 3.6.1–3.6.3, the integrated technology risk matrix (TRM) is used. The integrated TRM reflects an assessment of both the probability of technical failure P_f and the consequences of failure C_f, should it occur. Fig. 5 illustrates a generic version of the integrated TRM.

The integrated TRRA value I_{TRRA} is obtained for each removal method by summing the product of likelihood and consequence of failure of the three key technologies:

$$I_{TRRA} = \sum_{i=1}^{n} C_{f,i} \times P_{f,i} \tag{12}$$

where subscript i denotes the technology number, and n is the total number of technologies considered in the analysis ($n = 3$ in this work.)

3.7. Mission risk

The mission risk is concerned with the identification of any mission-specific failure modes that arise from the particular removal method. The risk assessment method utilized in this paper is based on models from Goddard Space Flight Center (GSFC) Risk Matrix Standard Scale [32]. Table 5 outlines the scales for mission failure likelihood P_{MR} and their consequence values C_{MR}. The overall expected percentage of unachieved mission objectives $\mathscr{E}_{MR}$ over a number of failure events (m) is calculated as follows:

$$\mathscr{E}_{MR}(\%) = \sum_{i=1}^{m} C_{MR,i} \times P_{MR,i} \tag{13}$$

In Table 5, the term "consequence" refers to the impacts of a failure on mission objectives, and "likelihood" refers to the estimated chance of not meeting performance requirements due to technical failures. To better indicate the failure likelihood, its 1-to-5 scale is mapped on to different ranges of *technical* risk P_T, which can be measured based on the probability of not meeting the minimum required technical performance in a mission or drifting from a specified performance margin [33].

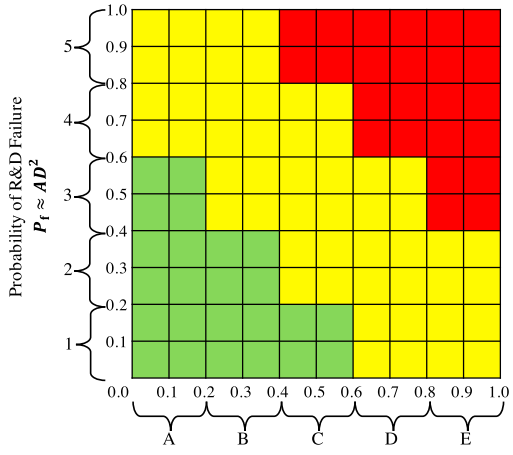

Probability Ratings (P_f)			Consequence Ratings (C_f)		
Level		Likelihood	Level		Impact
Quantitative	Qualitative		Quantitative	Qualitative	
0.0-0.2	1	Remote	0.0-0.2	A	Minimal
0.2-0.4	2	Unlikely	0.2-0.4	B	Some
0.4-0.6	3	Likely	0.4-0.6	C	Moderate
0.6-0.8	4	Highly Likely	0.6-0.8	D	Major
0.8-1.0	5	Near Certainty	0.8-1.0	E	Unacceptable

Fig. 5. Integrated technology risk matrix.

4. Debris removal methods

Since this study is focused on the active removal of large orbital debris, only the applicable methods are considered. Each method will be described briefly within the context of the criteria prescribed in Section 3. The advantages and disadvantages/challenges associated with each method are outlined. For each removal method, three risk factors are identified and explained, which are labelled by ℜ1 to ℜ3.

For the purpose of this study, each remover spacecraft is assumed to be equipped with two RIT-24 ion thrusters, with the exception of the ion-beam shepherd spacecraft that has three thrusters (two to navigate the remover, and one pointed at the debris for its deorbitation process). RIT-24 (by Airbus Defence & Space) uses xenon as propellant, requires 6 kW of power (nominal), and produces a thrust force of 200 mN at a specific impulse (I_{sp}) of 4300 s [34]. The mass of the thruster (without the power plant) is about 10.0 kg. Since the ion thruster is the most power-consuming component, the required power for each removal method is based on the thrusters power requirement, with the exception of the space-based laser method in which the laser instrument consumes considerable amount of electrical energy. The mass of the power plant accompanying the ion thruster is calculated from the following [35]:

$$m_{pow} = \frac{F_{th}\gamma I_{sp} g}{2\eta} \tag{14}$$

where $\eta = 90\%$ [36] is the thruster's efficiency and $\gamma = 10$ kg/kW [35] is the inverse specific power of the thruster. Using Eq. (14), the power plant mass per each RIT-24 ion thruster is estimated to be $m_{pow} = 60$ kg, resulting in a net mass of about 70 kg for the thruster and its power plant.

Further, the remover spacecraft in contact methods carry ad hoc devices that can be attached to the target debris to perform *controlled reentry* of the debris into the Earth's atmosphere, and land the debris in the South Pacific Ocean Uninhabited Area (SPOUA). These devices are considered to be chemical thrusters, known as the thruster deorbiting kits (TDK) [37], each having a mass of 100 kg [38]. Each TDK module is installed to the debris (Fig. 6) once the remover has transferred the debris to the 150-km deorbit altitude and prior to letting go of the debris. Since there are five debris to be removed, the initial overall mass of the remover spacecraft in each contact methods is increased by 500 kg to account for the mass of five TDK modules.

4.1. Throw nets

Capture by means of net devices is based on the deployment of nets around the target debris. Once the debris is surrounded, the net is closed and the debris is captured (Fig. 7). There are several advantages of using nets to collect and remove debris from space. Firstly, the spacecraft can stay at a relatively large distance from the target at the time of capturing, minimizing the risk of collision with the debris. Secondly, unlike other removal methods that require rigid contact, nets can be made of elastic materials which simplifies the requirements on precision. Thirdly, a single net can be used for debris with different sizes.

Several concepts have been proposed for ADR using nets, such as the Robotic Geostationary Orbit Restorer (ROGER) [40]. As the name suggests, ROGER is primarily proposed for the removal of dysfunctional satellites from GEO and transferring them to graveyard orbits. It can be similarly used for deorbiting large debris from LEO. The baseline spacecraft has a dry mass of 710 kg including 5 throw nets. Considering two RIT-24 thrusters and 5 TDK modules, the dry mass and power requirement of the modified system would be 1350 kg and 12 kW,

Table 5
Definition of risk matrix bins (adopted from Ref. [26]).

Consequence, C_{MR}					
Bin	A	B	C	D	E
Qualitative	Very low	Low	Moderate	High	Very High
Impact	minimal loss of mission objectives	small loss of mission objectives	moderate loss of mission objectives	significant loss of mission objectives	mission failure
Quantitative	1%	10%	50%	90%	100%
Likelihood, P_{MR}					
Bin	1	2	3	4	5
Qualitative	Very Low	Low	Moderate	High	Very High
Quantitative	$0.1\% < P_T \leq 2\%$	$2\% < P_T \leq 15\%$	$15\% < P_T \leq 25\%$	$25\% < P_T \leq 50\%$	$P_T > 50\%$

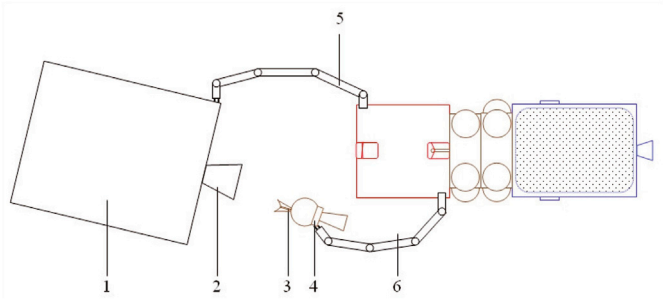

Fig. 6. TDK installation to the target debris [37]. 1: debris; 2: attachment location; 3: expandable umbrella; 4: TDK; 5 & 6: robotic arms.

ejected from the debris, it generates a momentum change similarly to the impulse delivered by a rocket. Generally, the momentum change is generated in the direction of the laser's incoming beam. The method provides contactless manipulation of space debris, which removes the requirement for complex contact and rendezvous operations. Debris removal using (space-based) lasers benefits from not requiring extra propellant dedicated to the alteration of debris trajectory during deorbitation, at the price of *uncontrolled* reentry of the debris. Also, many have voiced concerns over using, or misusing in fact, such high-power lasers in military applications (the so-called "weaponization of space" [41,42]), since it is powerful enough to vaporize debris, and therefore can interfere with other space assets in an aggressive manner. Further discussion of this matter is irrelevant to this paper and bears no technical value. On the technical side, the laser would need to be able to produce high power

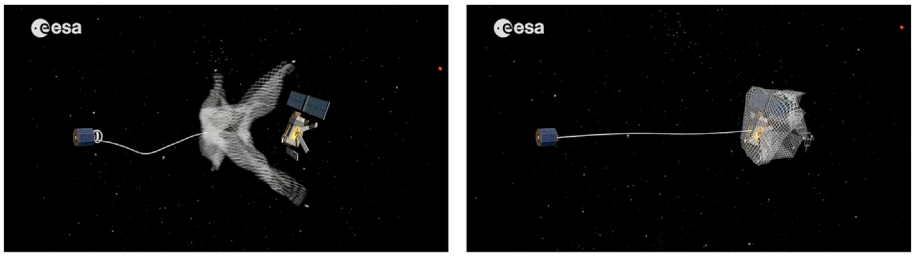

(a) Net deployed. (b) Target captured.

Fig. 7. ESA's e.Deorbit system study for active debris removal [39].

respectively.

One challenge associated with the net method is the potential risk of fragmentation of the debris (ℜ1), when the net surrounds and closes around the debris. This becomes especially important when the debris has large appendages such as solar arrays and antennas. Moreover, during the capturing phase, there will be shock and vibration loads exerted to the debris structure, which may not be fully *passivated*[1]. Hence, if there are any energy sources on board that are not fully depleted, the risk of explosion (ℜ2) exists, which can result in further fragmentation of the debris. Further, debris removal using nets suffers from a major drawback: the chance of missing (i.e., failure to capture) the target (ℜ3) during the capturing phase. This can result in mission failure since the mechanism is very difficult, if not impossible, to reuse.

4.2. Space-based lasers

The space-based laser method works based on the principle of the ablative laser propulsion, which relies on using a high-powered laser to ablate, a form of vaporization, the surface of the debris. As the vapor is ejected from the debris, it generates a momentum change similarly to the impulse delivered by a rocket. Generally, the momentum change is generated in the direction of the laser's incoming beam. The method provides contactless manipulation of space debris, which removes the requirement for complex contact and rendezvous operations. Debris removal using (space-based) lasers benefits from not requiring extra propellant dedicated to the alteration of debris trajectory during deorbitation, at the price of *uncontrolled* reentry of the debris. Also, many have voiced concerns over using, or misusing in fact, such high-power lasers in military applications (the so-called "weaponization of space" [41,42]), since it is powerful enough to vaporize debris, and therefore can interfere with other space assets in an aggressive manner. Further discussion of this matter is irrelevant to this paper and bears no technical value. On the technical side, the laser would need to be able to produce high power outputs, and would require high quality optics to filter and focus the beam on the debris.

When a laser pulse is incident on a target in vacuum, mechanical impulse is created by the pressure of photo-ablation at the target surface [43] (Fig. 8). The figure of merit for this interaction is the mechanical coupling coefficient, C_m, between the laser pulse and the debris surface. Typical values for C_m are in the order of 50–160 N/MW [44].

The total delta-v induced during the removal period by the laser system, Δv_{LSR}, can be calculated using the following:

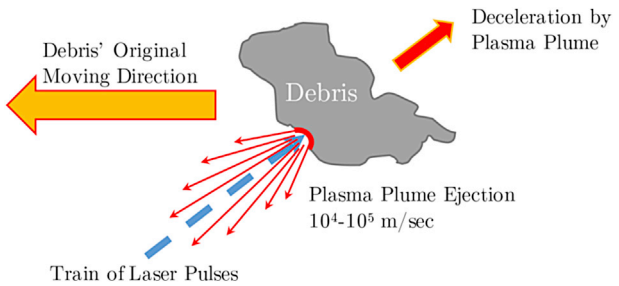

Fig. 8. Space debris is ablated after hitting by train of laser pulse [45].

[1] According to the debris mitigation guidelines published by IADC, passivation is defined as "the elimination of all stored energy on a spacecraft or orbital stages to reduce the chance of breakup. Typical passivation measures include venting or burning excess propellant, discharging batteries and relieving pressure vessels." [3].

$$\Delta v_{\mathrm{LSR}} = \sum_{j=1}^{n} \frac{C_{\mathrm{m}} E}{m_j} \tag{15}$$

where E is the energy of the incident pulse, and m_j is the mass of debris after bombardment by j pulses:

$$m_j = m_{\mathrm{deb}} - \sum_{i=1}^{j} \Delta h E \tag{16}$$

where Δh is the ablation rate. For aluminium, $\Delta h = 90 \times 10^{-9}$ kg/J.

For the purpose of this study, the simulation parameters will be based upon the L'ADROIT [44] laser system. The system provides 40 kW bursts of 100 ps, 355 nm ultraviolet pulses, with 1950 J energy per pulse. (UV wavelength is not a hazard to other space-based sensors, nor to people on Earth [44].) The total dry mass of the system is estimated to be 8640 kg, of which 8500 kg is the mass of the L'ADROIT spacecraft and laser system, and 140 kg is for two RIT-24 thrusters. The total system electrical power requirement is estimated to be 67 kW (data acquired from Table B2 in Ref. [44]). Since the method does not physically contact the debris and does not provide controlled reentry, TDK modules are not required.

Some studies suggest that the laser method may suffer from thrust degradation due to the attenuation of the laser beam by ejecta plume. The attenuation can be due to two major factors: a) the effect of ejecta on the laser optics, solar panels, etc., and b) mechanical interfere between the ejecta plume and the incoming laser beams, regardless of the source proximity, absorbing some energies of the beams and hence causing a degradation in the amount of energy that is transferred by the laser beams [46,47]. Since the LSR spacecraft stays at far distances from debris objects, the deposition of ejecta particles on the laser optics and solar panels is not applicable in this work. However, mechanical interference of the ejecta with the laser beams has been considered as (ℜ1) in this study.

Another possible risk is the high temperature of the ablation spot, which reaches 4285–4747 K [46]. Such high temperatures may lead to the explosion of non-empty propellant tanks or other energy storage devices that are not properly insulated (ℜ2). Lastly, the LSR's vision system may not be able to perform rapid target detection, acquisition, and tracking from such far distances [48–50], and hence the mission may be delayed (ℜ3).

4.3. Ion beam shepherd

The ion beam shepherd (IBS) method is another contactless approach in which a hovering spacecraft (called *shepherd*) exerts a thrusting force on the debris by producing highly collimated, high-velocity ion beam directed against the debris to modify its orbit and/or attitude [51,52], through the momentum carried by plasma ions and transmitted to the target debris (Fig. 9). The shepherd spacecraft is equipped with a secondary propulsion system that produces an equilibrium force to keep the shepherd and debris at constant distance, and a radar to monitor and estimate the position of the target continuously.

Based on the assumptions that the debris orbit is initially circular and that it undergoes a constant tangential acceleration, the time required to transfer the debris to the deorbit altitude, $\Delta t_{\mathrm{do}}^{\mathrm{IBS}}$, is calculated from the following [53]:

$$\Delta t_{\mathrm{do}}^{\mathrm{IBS}} = \frac{m_{\mathrm{deb}} \Delta v_{\mathrm{do}}}{\eta_{\mathrm{beam}} F_{\mathrm{th}}} \tag{17}$$

where Δv_{do} is obtained from Eq. (1a), and η_{beam} is the beam momentum transfer efficiency, which depends primarily on the beam-target interaction geometry [53]. In this study, a beam efficiency of $\eta_{\mathrm{beam}} = 70\%$ will be considered. The shepherd spacecraft is equipped with three RIT-24 ion thrusters with the total required power of 18 kW. Of the three thrusters, two are utilized to navigate the remover, and one is pointed at the debris for the deorbitation process. The dry mass of the spacecraft is taken to be 910 kg of which 700 kg is the mass of the baseline spacecraft system and 210 kg is the mass of three thrusters plus their power plants. Similarly to the laser method, since the method does not physically contact the debris and does not provide controlled reentry, TDK modules are not required.

The main advantage of the IBS method is that since it does not require docking with the target, its operation is independent of the debris' attitude dynamics. In terms of risks, the shepherd spacecraft is required to keep a safe distance from the target debris at all times during the removal operation in order to avoid any collisions. Failure to do so should most likely result in catastrophic accident (ℜ1) and loss of mission. Further, the misalignment between ion beam center of pressure and target's center of mass can result in an excessive spin-up of the target that could pose risks such as fragmentation of the target due to centrifugal forces (ℜ2). Moreover, the secondary ions backscattered from the target surface impose the possible risk of contamination of sensitive parts of the shepherd spacecraft (ℜ3), such as solar panels and cameras.

4.4. Electrodynamic tethers

In principle, the electrodynamic tether (EDT) is a form of space propulsion system, based on the exploitation of the Lorentz force due to the interaction between the electric current flowing in a conductive tether and the geomagnetic field (Fig. 10).

The total time required for an EDT system to deorbit a debris, $\Delta t_{\mathrm{do}}^{\mathrm{EDT}}$, can be approximated by Ref. [55]:

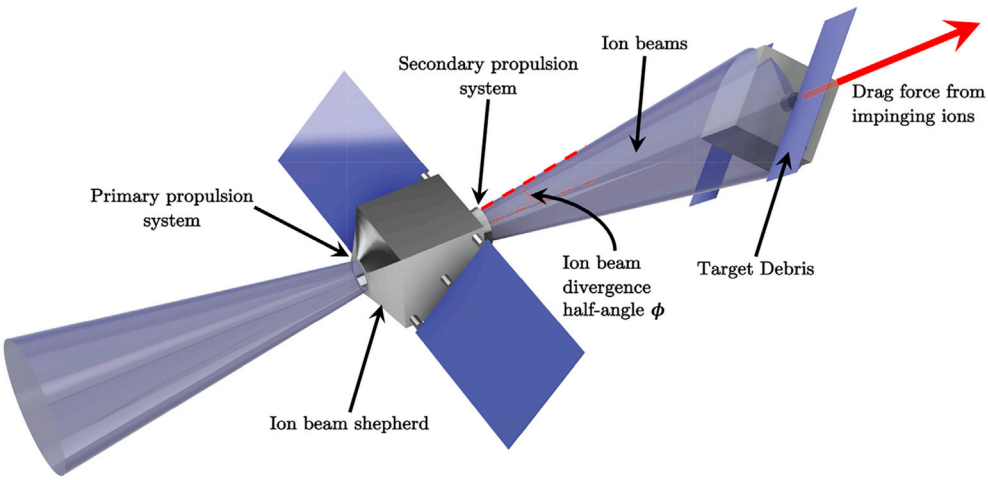

Fig. 9. Schematic of ion beam shepherd spacecraft deorbiting a space debris.

$$\Delta t_{\mathrm{do}}^{\mathrm{EDT}} = \frac{m_{\mathrm{sys}} R_{\mathrm{tether}}}{12 L_{\mathrm{tether}}^2 B_{\oplus}^2 R_{\oplus}^6 \cos^2\alpha \langle \cos^2\lambda \rangle} \left(r_{\mathrm{deb}}^6 - r_{\mathrm{do}}^6 \right) \tag{18}$$

R_{tether} is the total resistance of the tether system (including tether, control circuit, plasma contact, and parasitic resistances), L_{tether} is the tether's length, $B_{\oplus} = 31\ \mu$T is the strength of the magnetic field on the magnetic equator at the surface of the Earth, α is the angle between the tether and the local vertical, and [55].

$$\left\langle \cos^2\lambda \right\rangle = \frac{1}{16}(6 + 2\cos 2i + 3\cos(2(i-\phi)) + 2\cos 2\phi + 3\cos(2(i+\phi))) \tag{19}$$

is the average of $\cos^2\lambda$ as λ (the inclination of the spacecraft orbit with respect to the geomagnetic frame [55]) varies over one day due to Earth's rotation. In Eq. (19), i is the orbit inclination and $\phi \approx 11.5^\circ$ is the angle between the axis of rotation of Earth and its dipole axis. Further, to account for the variation in tether attitude, it is assumed that the tether is aligned off the local vertical at a mean angle of $\alpha = 35^\circ$.

The tether resistance can be scaled with tether length [56] through resistivity ρ such that $R_{\mathrm{tether}} = \rho L/A$, where A is the cross-sectional area of the tether. For the purpose of this study, it will be assumed that the tether is made of aluminum with $\rho = 2.82 \times 10^{-8}$ ohm-m, and has a diameter of 3 mm. Based on the Terminator Tether™ model [55,57], it is assumed that the tether can extend up to 10 km a 10-km long aluminum tether with a diameter of 3 mm would have a mass close to 200 kg. Further, considering another 50 kg for the accompanying power avionics and mechanical structures, the overall mass of the tether is assumed to be 250 kg. The remover spacecraft is selected to be the modified Deutsche Orbitale Servicing Mission (DEOS [58]) spacecraft (described in Section 4.5), equipped with and EDT module that is used during the deorbitation process. The initial total dry mass of the remover spacecraft is estimated to be about 1605 kg, with the following breakdown: 670 for the DEOS spacecraft, 250 kg for the EDT module, 45 kg for the second robotic arm [37], 140 kg for two RIT-24 ion thrusters, and 500 kg for 5 TDK modules.

An advantage of the EDT system is that it can generate thrust for very long duration with little or no consumption of expendables. However, it requires rigid contact with the target debris in first place. This is a big disadvantage and imposes risks to mission success. Failure to capture the debris or to maintain the contact with the debris (ℜ1) is a clear mission risk. Moreover, the length of the tether in the EDT system must be in the orders of several kilometers to produce considerable amount of thrust (or drag). As a result, there is the risk of collision between the tether and other operating spacecraft or debris (ℜ2–see Refs. [59,60], for example, for the extended discussions of the mentioned risk), which could affect debris population adversely. Further, when the EDT module is deployed, a very long non-rigid structure is formed which can get tangled or become damaged and disconnected (ℜ3) during the mission (as experiments in the STARS-11 mission [61] suggested).

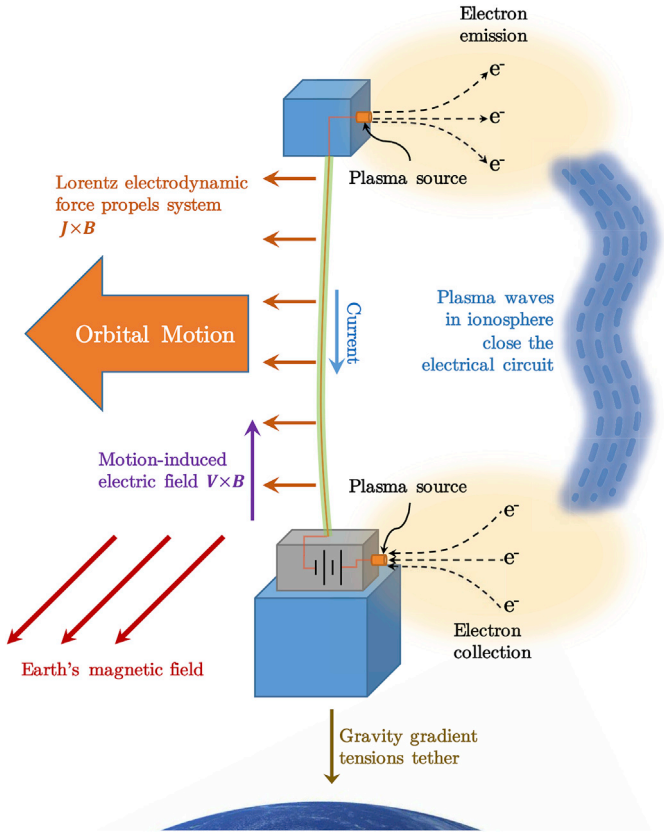

Fig. 10. The essential physics of EDT propulsion (Image replicated from Ref. [54]).

4.5. Robotic arm

One of the most studied ADR techniques is the removal by means of robotic arms. In this approach, the remover spacecraft that is equipped with one or more robotic manipulators approaches the target debris, grapples it, and deorbits it. In the literature (e.g. [62,63]), robotic manipulators have been suggested and widely studied for in-orbit servicing and refueling operations. One example is the Deutsche Orbitale Servicing Mission (DEOS)–a technology demonstration mission that was planned for 2018 but now is canceled. The primary goal of DEOS was to capture an uncooperative satellite and move it safely to a predefined Earth orbit. Eventually, the rigidly-coupled spacecraft were to re-enter the atmosphere, and consequently disintegrate and burn up [64]. Fig. 11 shows the artist's rendition of the DEOS mission scenarios. The DEOS spacecraft is reported to have a dry mass of 670 kg with an average power of 1 kW [58]. Considering that the spacecraft is equipped with two RIT-24 ion thrusters (140 kg), a secondary robotic arm (45 kg), and 5 TDK modules (500 kg), the dry mass of the system and the required power would increase to 1355 kg and about 12 kW, respectively.

Similarly to the EDT method, the robotic arm removal method requires rigid contact with the uncooperative target. Such requirement imposes the risk of creating more debris due to fragmentation (ℜ1) of the target at the instant of contact. Also, if the relative attitude rate between the two spacecraft is large enough, the robotic manipulator can be damaged. In addition, in case of high relative attitude rates the convergence of orbital and attitude controls for rendezvous and capture may not be guaranteed (ℜ2), and hence mission success can be adversely affected. Lastly, failure to capture the target debris (ℜ3) successfully is another risk

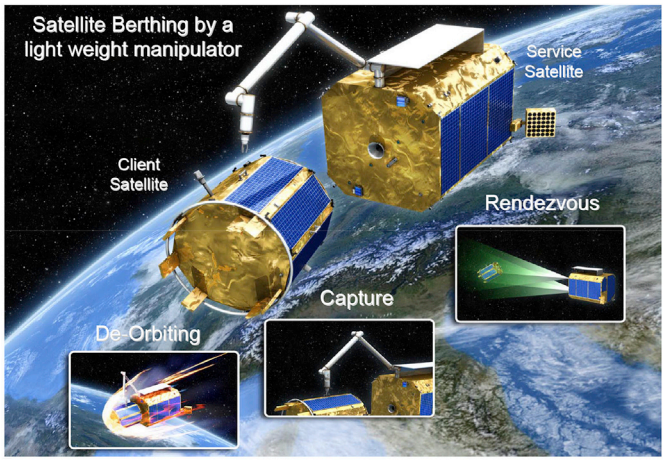

Fig. 11. Deutsche Orbitale Servicing Mission (Image credit [64]).

that must be addressed. This is a common concern regarding both removal by nets and robotic manipulators. However, the consequence of such event on the mission success in the latter method is not as adverse as it is in the former one. This is because a robotic manipulator can attempt to capture a target debris several times given that no incident occurs.

5. Removal scenarios

Table 6 summarizes the removal methods selected for this study, as well as the maneuvers required to accomplish the mission. For all methods, it is assumed that the remover spacecraft is initially launched and inserted into the orbit of the first target debris.

In the EDT and ARM methods, the remover spacecraft performs phasing maneuver with the target debris, synchronizes its rotational state with that of the debris, captures and detumbles the debris, and then moves the debris to the deorbit altitude. In the EDT method, the deorbitation is performed using the EDT module, and in the ARM method using the ion thrusters. Once deorbitation is complete, the remover spacecraft in both methods install TDK modules to the debris. Then the remover let go of the composite system for the controlled reentry process. Fig. 12 summarizes the steps pictorially.

The process in the NET method is very similar to EDT and ARM. However, since the debris detumbling requirement in the NET method is not as strict as it is in the EDT and ARM methods, a partial detumbling of the debris is presumed for NET.

In the IBS method, the remover spacecraft is not required to perform any proximity maneuvers. Also, the ion thrusters are used to adjust the spacecraft orbit and to lead the target from a safe distance. Upon deorbiting the target, the remover spacecraft moves to the orbit of the next target and repeats the process.

In the LSR method, the laser-laden spacecraft is assumed to be able to shoot laser pulses at the debris from a 1000-km distance [44]. As such, if the remover spacecraft is in an orbit that is 1000 km (or less) smaller or larger than the target debris, it does not need to change its semi-major axis. Further, the difference in the inclination of the remover spacecraft's orbit and that of the target debris is allowed to be as much as 90°, i.e., no orbital change maneuver is required. To account for the occultation of the debris from LSR spacecraft's view (i.e., Earth blocks from the view (occults) the debris), and to account for the fact that the remover needs to *lead* the debris so that the laser pulses reduce the debris' altitude, a 50% duty cycle will be assumed for the operation of the laser.

6. Evaluation of assessment criteria

In this section, the attributes used in the assessment are evaluated. The removal timeframe and performance robustness are obtained using the Monte Carlo simulation while the remaining attributes are obtained using values and relationships outlined in Section 4. The preliminary results are presented in Tables 7–11.

Table 6
Active debris removal methods considered in this study and the required maneuvers.

	Tether	Space	Ion-Beam	Electrodynamic	Robotic
	Net	Laser	Shepherd	Tether	Arm
Abbreviation	NET	LSR	IBS	EDT	ARM
SMA Change	Yes	Partial[a]	Yes	Yes	Yes
Inclination Change	Yes	No	Yes	Yes	Yes
RAAN Correction	Yes	No	Yes	Yes	Yes
Orbit phasing	Yes	No	Yes	Yes	Yes
Synchronization	No	No	No	Yes	Yes
Capture	Yes	No	No	Yes	Yes
De-tumble	Partial[b]	No	No	Yes	Yes
TDK attachment	No[c]	No	No	Yes	Yes

[a] Required if debris orbit is over 1000 km smaller/larger than the LSR orbit.
[b] See Ref. [65].
[c] TDK modules are assumed to be built in the net mechanisms.

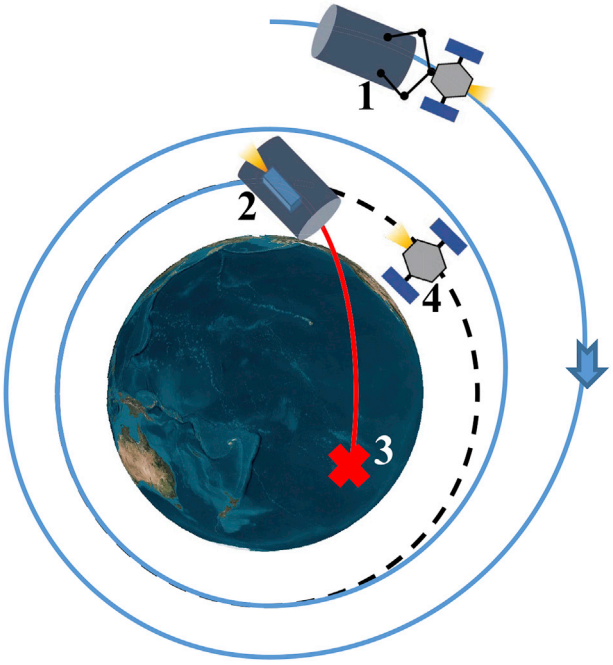

Fig. 12. 1) Remover spacecraft performs deorbitation; 2) TDK puts the debris on the controlled reentry trajectory; 3) Debris and TDK crash within SPOUA; 4) Remover moves on to the next debris. Blue line: deorbit trajectory; Blue arrow: orbital motion direction; dashed line: deorbit altitude; red line: reentry trajectory, Red "X": impact zone. (For interpretation of the references to colour in this figure legend, the reader is referred to the Web version of this article.)

6.1. Removal time & performance robustness

The removal time for each method is determined directly from the Monte Carlo simulation. In total, 1000 debris removal scenarios are created, wherein 5 randomly selected debris are deorbited from their initial orbit. The average value of the removal times over 1000 simulation runs and the coefficient of variation are listed in Table 7. It should be noted that a lower coefficient of variation indicates a higher performance robustness.

6.2. Propellant mass

In all methods but LSR, the remover spacecraft utilizes its ion thrusters to rendezvous with the debris. In NET and ARM, ion thrusters are used to transfer the combined remover and debris system during the deorbiting maneuver. Therefore, the total mass of the system during the deorbitation is equal to the remover spacecraft mass plus the debris mass. In the LSR method, the remover is assumed to be capable of shooting laser pulses from afar, up to 1000 km away, and without requiring to

Table 7
Average time for removal of 5 debris obtained from the Monte Carlo simulation.

Variable	NET	LSR	IBS	EDT	ARM
$\bar{t}_{sma}$ (days)	84.11	36.58	71.11	103.03	89.84
$\bar{t}_{inc}$ (days)	418.43	0.0	361.62	517.10	442.35
$\bar{t}_{raan}$ (days)	586.21	0.0	488.32	716.53	631.05
$\bar{t}_{ph}$ (days)	6.59	0.0	5.65	8.09	7.01
$\bar{t}_{prx}$ (days)	30.33	0.00	0.00	110.87	259.33
$\bar{t}_{do}$ (days)	283.43	680.04	473.60	556.72	292.18
Δt_{rmv} (days)	1409.10	716.61	1400.30	2012.33	1721.76
$\sigma_{t_{rmv}}$ (days)	320.54	108.60	400.03	850.43	310.54
$c_{t_{rmv}}$	0.2891	0.0980	0.1782	0.2043	0.2928

Table 8
Consumed propellant for the removal of 5 debris obtained from the Monte Carlo simulation.

Variable	NET	LSR	IBS	EDT	ARM
$\overline{m}_{\text{sma}}$ (kg)	69.39	220.00	59.08	85.00	89.84
$\overline{m}_{\text{inc}}$ (kg)	352.15	0.0	306.58	435.21	442.35
$\overline{m}_{\text{raan}}$ (kg)	470.86	0.0	394.51	575.24	631.05
$\overline{m}_{\text{ph}}$ (kg)	4.70	0.0	5.65	5.77	7.01
$\overline{m}_{\text{prx}}$ (kg)	21.27	0.0	0.00	211.33	259.33
$\overline{m}_{\text{do}}$ (kg)	223.24	0.0	473.60	0.0	292.18
$\overline{m}_{\text{prp}}$ (kg)	1141.61	220.00	1037.47	1312.55	1721.76
$\sigma_{\overline{m}_{\text{prp}}}$ (days)	320.54	23.54	400.03	850.43	310.54

Table 9
Parameters used in the CER QuickCost model and estimated cost in FY2020. ATP year: 2005; Planetary: 0; Team: 2; Data: 50%; Inflation factor relative to the FY2010: 1.2179.

Variable	NET	LSR	IBS	EDT	ARM
Dry Mass (kg)	1350	8640	910	1605	1355
Power (kW)	12	64	18	12	12
Life (Months)	47	180	47	67	57
New	40%	60%	50%	70%	20%
InstCompl%	20%	70%	50%	70%	30%
$\mathscr{D}$ ($M)	279.7	257.9[a]	333.3	629.1	257.7
$\mathscr{I}$ ($M)	50.0	173.8	39.2	58.4	54.5
$\mathscr{T}$ ($M)	374.48	473.00	425.86	788.17	353.49

[a] Correction factor applied. See the text for discussion.

Table 10
Allocated TRRA attributes (AD^2 values adopted from Refs. [56,66]).

Method	Technology	TRL	TNV	AD^2	C_f	P_f
NET	T1. Net & ejector systems [38]	5	5	2	1.2	2
	T2. Target debris attitude rates determination system [65,67]	4	4	7	2	7
	T3. Proximity formation flying GNC [68]	5	3	4	0.8	4
$I_{\text{TRRA}} = 1.76$						
LSR	T1. Laser [68]	3	5	7	3.6	7
	T2. Power storage [69]	5	5	6	1.2	6
	T3. Optical sensors for debris detection/tracking [68]	7	5	2	0	2
$I_{\text{TRRA}} = 3.12$						
IBS	T1. Ion Thruster [68]	4	5	5	2.4	5
	T2. Propellant storage [70]	7	2	3	0	3
	T3. Proximity formation flying GNC [68]	5	3	4	0.8	4
$I_{\text{TRRA}} = 1.20$						
EDT	T1. Tether system [37]	3	5	6	3.6	6
	T2. Target debris attitude rates determination [65,67]	4	4	7	2	7
	T3. Power storage [69]	5	5	6	1.2	6
$I_{\text{TRRA}} = 3.80$						
ARM	T1. Robotic manipulator	7	5	1	0	1
	T2. Target debris attitude rates determination [65,67]	4	4	7	2	7
	T3. Proximity formation flying GNC [68]	5	4	5	1	5

$I_{\text{TRRA}} = 1.80$.

correct its inclination or RAAN. As such, very small amount of propellant is consumed to correct remover's orbit. In the IBS method, while the tertiary thruster is used to deorbit the debris, the primary and secondary thrusters are used to "lead" the debris to the deorbit altitude. As a result, during the deorbitation, the total consumed propellant is the sum of propellant mass used by all three thrusters. Lastly, in the EDT method, since the source of thrust on the debris is the Lorentz force, no propellant is expended during the deorbitation process. Table 8 summarizes the average propellant mass used during each maneuver. The results clearly show that a considerable amount of propellant is consumed during the RAAN correction, inclination change, and deorbiting maneuvers. While the third is due to the large mass of the debris-remover composite system, the first and second are due to the very large delta-v requirement of the maneuvers.

Table 11
Allocated mission risk attributes.

Method	Mission Risk Description	C_{MR}	P_{MR}
NET	ℜ1. Explosion of debris energy stores and further fragmentation [38]	*E*	2
	ℜ2. Damages to the remover spacecraft due to uncontrolled debris attitude rates [71]	*D*	2
	ℜ3. Debris capturing is unsuccessful [71]	*D*	3
	$\varepsilon_{\text{MR}} = 51.0\%$		
LSR	ℜ1. Thrust degradation due to attenuation of the laser beam caused by the ejecta plume [46]	*B*	5
	ℜ2. Explosion of debris energy stores and further fragmentation due to extremely high temperature created during ablation [72]	*E*	3
	ℜ3. Vision system fails to detect, acquire, and track the target debris [48,73]	*C*	3
	$\varepsilon_{\text{MR}} = 45.0\%$		
IBS	ℜ1. Shepherd fails to keep a safe distance from the target and collides with it [35]	*D*	2
	ℜ2. Fragmentation of target due to excessive spin-up resulting from misalignment between ion beam center of pressure and target center of mass [52]	*E*	2
	ℜ3. Secondary ions backscattered from the target surface contaminate sensitive parts [52]	*C*	4
	$\varepsilon_{\text{MR}} = 53.5\%$		
EDT	ℜ1. Explosion of debris energy stores and further fragmentation [38]	*E*	2
	ℜ2. Tether gets tangled or collides with other in-orbit objects and creates more debris [74,75]	*E*	2
	ℜ3. Debris capturing is unsuccessful [37]	*C*	4
	$\varepsilon_{\text{MR}} = 55.0\%$		
ARM	ℜ1. Explosion of debris energy stores and further fragmentation [38]	*E*	2
	ℜ2. Damages to remover spacecraft due to uncontrolled debris attitude rates [76]	*D*	3
	ℜ3. Debris capturing is unsuccessful [77]	*C*	4

$\varepsilon_{\text{MR}} = 62.5\%$

6.3. Mission cost

The non-recurring cost for development plus one qualification unit for each removal method is estimated based on the parameters pertaining to the existing concepts, or the proposed ones. The parameters of each removal method that is relevant to the cost estimation were introduced in Section 4. The result of the cost estimation along with the attributes used in the analysis are presented in Table 9.

In Table 9, the values assigned to *Dry Mass* and *Power* were discussed in Section 4. The value assigned to the *Life* attribute is equal to the removal time, Δt_{rmv}, from Table 7 (expressed in months), with the exception of the LSR method. Since the LSR spacecraft has the potential to stay much longer in orbit (10–15 years) and remove several more debris during its lifetime, it would be financially and technologically unjustifiable to terminate the LSR mission after the removal of only 5 debris (which is computed to take about 24 months). Therefore, to account for LSR mission extendability potential, the cost of development, $\mathscr{D}$, is scaled for LSR in this study. For that, the LSR mission lifetime is initially considered to be 180 months, which yields to a development cost of $\mathscr{D} = \$1,934.5$ million, and then the *scaled* development cost is obtained by applying a correction factor to $\mathscr{D}$. The factor is obtained by dividing the number of months it takes LSR to remove 5 debris (i.e., 24 months) by LSR's potential mission lifetime (i.e., 180 months): $24/180 \approx 0.13$.

6.4. Technology readiness and risk

This paper considers the TRL level of the three primary technologies for each removal method. The assigned values for TRRA are presented in

Table 10. The TRL values are acquired through the evaluation of the state-of-the-art technologies available in the literature. The references provided for each technology and risk provide some insight into the values assigned to each method.

6.5. Mission risk

Three major mission risks associated with each removal method are considered in the study, which were explicitly outlined in Section 4. The assigned values for the mission risk parameters are presented in Table 11. The values are adopted from references that are listed in each entry of the table.

7. Assessment techniques

To examine the viability of the removal methods, three distinct assessment techniques are utilized, and they are detailed in the following:

7.1. Analytical hierarchy process

The Analytical Hierarchy Process (AHP) is a multi-criteria decision-making approach, which makes pairwise comparisons between the decision alternatives to define their relative preference values with respect to each criterion, as well as pairwise comparisons between the criteria to define their relative importance values, in order to assign an overall decision value to each alternative [78]. In this study, the relative preference value for each pair of methods with respect to a particular assessment criterion is obtained by taking the ratio of their associated values of the assessment criterion, such that a ratio of bigger than one indicates a higher preference for the better method considering the specific criterion. For example, the relative preference between NET and ARM methods with respect to the removal time criterion is obtained by taking the ratio of $\bar{t}_{\text{rmv}}$ of ARM and that of NET, both of which were presented in Table 7. The ratio is greater than 1, which reflects the higher preference of NET method compared to ARM in the removal time criterion.

The relative preference values for the removal methods with respect to criterion k can be organized using a matrix, so that r_{ij}^k represents the preference of method i over method j. For each criterion k, to determine the overall relative preference of method i, R_i^k, each relative preference r_{ij}^k is first normalized with respect to its column, as follows:

$$r_{ij}^{'k} = \frac{r_{ij}^k}{\sum_{i=1}^{n} r_{ij}^k} \tag{20}$$

where n is the number of methods ($n = 5$ in this work). Then, by taking the average of normalized relative preferences in each row, the overall relative preference R_i^k with respect to criterion k can be obtained, as follows:

$$R_i^k = \frac{1}{n}\sum_{j=1}^{n} r_{ij}^{'k} \tag{21}$$

The relative importance between the assessment criteria is defined based on an eight-point ranking scale, where a value of 1 means least important, a value of 8 means most important, and the intermediate values. The assignment of rank to each criterion depends on whether a higher emphasis is on mission costs or on performance. In the former case, i.e., *cost-based*, the importance of assessment criteria is ordered, from highest to lowest, as: total mission cost (AC-5), removal time (AC-1), propellant mass (AC-4), average required power (AC-6), technology readiness and risk (AC-7), mission risk (AC-8), controlled re-entry (AC-03), and performance robustness (AC-2). In the latter case, i.e., *performance-based*, the order is as follows: performance robustness (AC-2), controlled re-entry (AC-3), technology readiness and risk (AC-7), mission risk (AC-8), removal time (AC-1), mission cost (AC-5), propellant mass (AC-4), and average required power (AC-6). A third approach is utilized to take a middle ground between the extremes presented in the two former approaches. In this case, called the *balanced* approach, the importance of each criterion is determined by taking the average rank of that criterion in the cost-based and performance-based approaches. Table 12 summarizes the importance value of each criterion in the three approaches. Similarly to the relative preferences, the relative importances are obtained by taking the ratio of the importance values of assessment criteria.

For each approach, the relative importance values can form a matrix, and they can be normalized to define an overall importance value O^k for criterion k, similarly to Eqs (20) and (21). To find the AHP score for each method i, A_i, the overall relative preference and importance values are then aggregated using the following:

$$A_i = \sum_{k=1}^{m} R_i^k O_i^k, \quad \text{for } i = 1, \ldots, n \tag{22}$$

where m is the number of criteria in the assessment ($m = 8$ in this work.)

7.2. Utility-based approach

Utility is defined as a measure of the worth of the attributes of a design or decision making process [79]. In this work, the attributes are the assessment criteria, as listed in Table 3. These criteria have been quantified for each debris removal method, and their values were shown in Tables 7–11. In the utility-based decision making, for each criterion a utility function is defined, which maps the physical range of the criterion onto the normalized range of 0–1. This will allow for the aggregation of the criteria based on their worth, instead of their physical values. Consequently, an overall worth can be associated to each debris removal method, and compared with that of other methods. The assignment of such utility functions is mostly done heuristically. Given that the intention in this work is to assess the relative value of certain debris removal techniques with respect to each other, it is reasonable to assume that for each criterion the maximum or minimum values obtained from all methods can indicate the highest or lowest worth of the criterion. Therefore, each utility function can be profiled using a normalized parameter s defined as:

$$s = \frac{x - x_{\min}}{x_{\max} - x_{\min}} \tag{23}$$

where x is the value of the criterion, and $x_{\min}$ and $x_{\max}$ are the minimum and maximum values of the criterion considering all the debris removal methods, respectively. The values of $x_{\min}$ and $x_{\max}$ can be obtained from Tables 7–11 Fig. 13 shows the parametric form of utility functions. Certain considerations have been made for defining the parametric forms. For example, when comparing Fig. 13(d) and (f), it can be verified that the utility function of the propellant mass criterion decreases faster than that of the required power criterion. This is because electrical energy can be generated by the spacecraft solar panels, whereas the exhausted propellant cannot be replaced conveniently.

In this assessment, the relative weights used in the utility-based approach are the same as the relative importance values defined in the AHP approach. Therefore, the aggregated utility value for each method i, U_i, can be obtained using the following:

Table 12
Importance value of each criterion based on three different assessment approaches.

Approach	AC-1	AC-2	AC-3	AC-4	AC-5	AC-6	AC-7	AC-8
Cost-based	7	1	2	6	8	5	4	3
Perf-based	4	8	7	2	3	1	6	5
Balanced	8	5	2	3	8	1	8	5

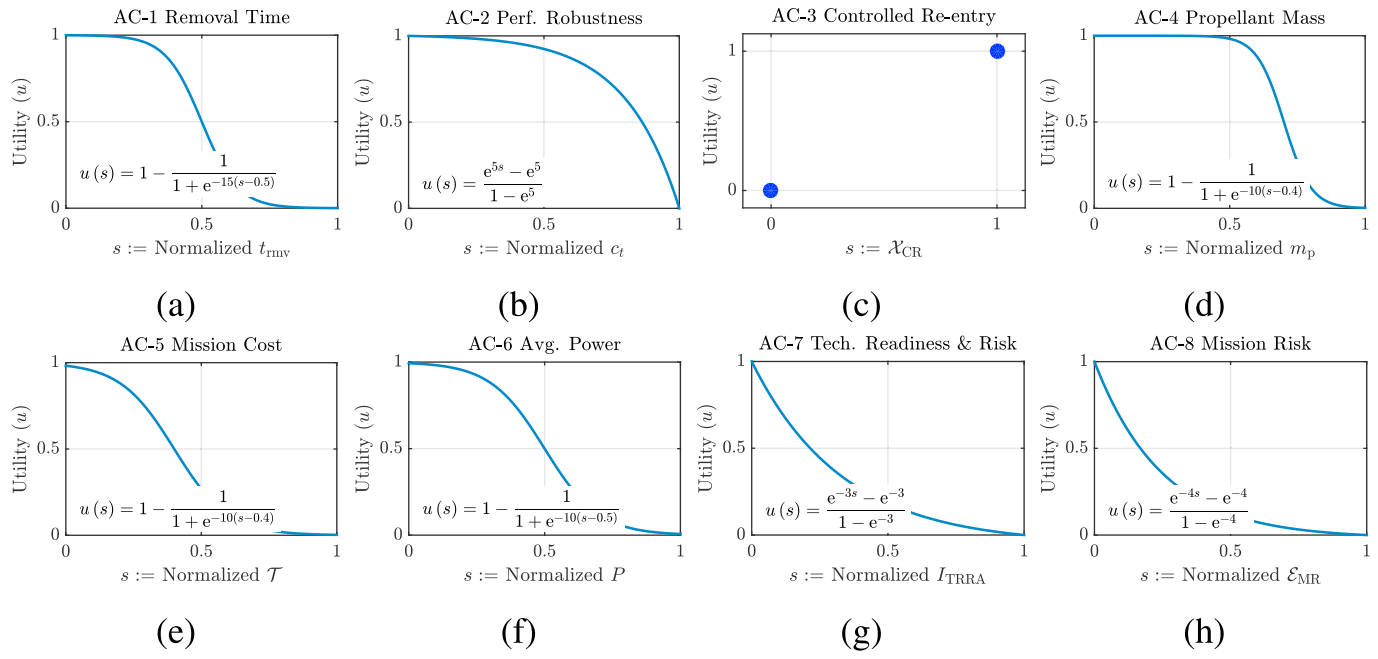

Fig. 13. Assigned utility function for each assessment criterion.

$$U_i = \sum_{k=1}^{m} O_i^k u_i^k, \quad \text{for } i = 1, \ldots, n \tag{24}$$

8. Results and discussions

A brief discussion of the results from each assessment will be discussed in this section, followed by a general overall evaluation of the results.

8.1. AHP-based performance comparison

As discussed in Section 7.1, the preference of a removal method over the other with respect to a criterion is obtained by taking the ratio of their associated values. The overall preferences are obtained using Eq. (21), and they are listed in Table 13. Fig. 14 shows the unweighted overall preference scores. The figure demonstrates that each removal method has its own strengths and weaknesses, and that its performance varies with respect to different criteria. LSR outperforms other methods in a number of criteria: removal time, performance robustness, propellant mass, and mission risk. The method greatly benefits from being able to shoot laser pulses at debris objects from 1000-km away, regardless of the orbit inclination differences. The IBS method performs well in technology readiness and risk criterion and it has the smallest I_{TRRA} value. NET, ARM, and EDT show similar performances in the controlled reentry criterion (all three methods carry TDK modules which can reenter debris in a controlled manner) as well the required power criterion (all three methods use 2 ion thrusters). Further, NET and ARM demonstrate acceptable and similar performances in a number of criteria, such as removal time, propellant mass, and the total mission cost. It should be noted that although the EDT method does not expend any propellant during the deorbitation process, the high mass of the tether system (and its power plant) adversely affect the performance of EDT in the propellant mass criterion and places the method on a par with NET.

Table 13
Normalized relative preferences for each criterion in AHP analysis.

	AC-1	AC-2	AC-3	AC-4	AC-5	AC-6	AC-7	AC-8
NET	0.18	0.20	0.33	0.11	0.24	0.26	0.22	0.21
LSR	0.36	0.29	0.00	0.58	0.19	0.05	0.13	0.23
IBS	0.18	0.16	0.00	0.12	0.21	0.17	0.33	0.20
EDT	0.13	0.11	0.33	0.10	0.11	0.26	0.10	0.19
ARM	0.15	0.25	0.33	0.09	0.25	0.26	0.22	0.17

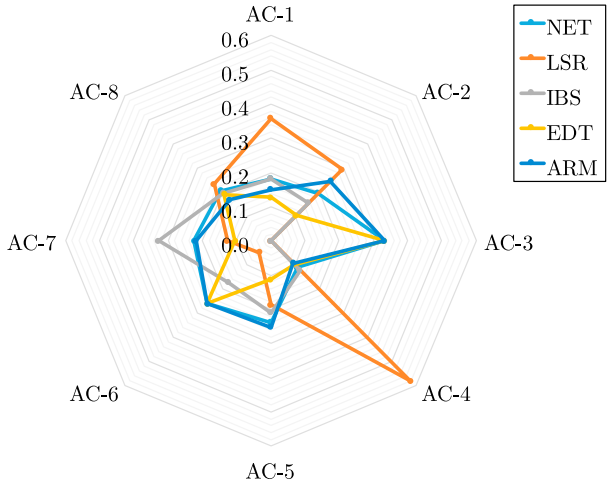

Fig. 14. Unweighted AHP scores of the removal methods.

While the unweighted AHP scores demonstrate the suitability of each method relative to certain criteria, in order to draw a final conclusion on the best method, one should apply the importance ranks of each criterion and aggregate the overall preferences of each method. The weighted overall preference of the removal methods are shown in Fig. 15. Based on the figure, LSR has the best performance in the cost-based approach (AHP score = 0.2559), followed by the NET method (AHP score = 0.2090) and ARM method (AHP score = 0.2004). In the performance-based approach, ARM has the best performance (AHP score = 0.2296), followed by NET (AHP score = 0.2279) and LSR (AHP score = 0.2079). In the balanced approach, LSR again outperforms other methods (AHP score = 0.2328), followed by NET (AHP score = 0.2196) and ARM (AHP score = 0.2172). In the contactless methods category, LSR clearly outperforms IBS in all three approaches.

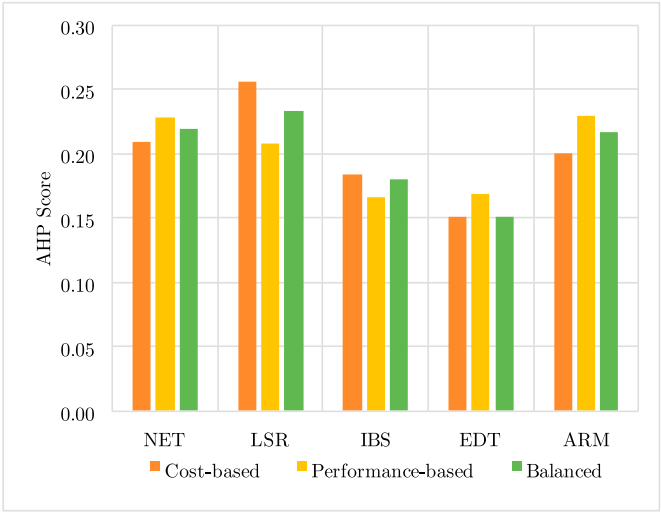

Fig. 15. Assessment result from AHP analysis.

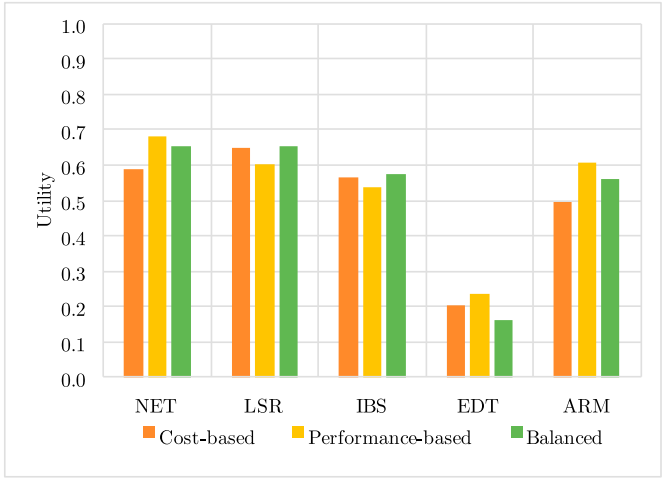

Fig. 16. Result of the utility-based analysis.

8.2. Utility-based performance comparison

The normalized parameter s obtained for each criterion and the associated *unweighted* utility values $u(s)$ are presented in Table 14.

The results of the weighted utility-based assessment are presented in Fig. 16. The figure clearly shows that LSR, NET, and IBS perform well in the cost-based approach, with utility values greater than 0.5, while ARM exhibits an average performance and the EDT method shows poor performance. The EDT method is highly disadvantaged by the required mass of the laser-laden spacecraft. As the results from the mission cost analysis showed (Table 9), the EDT mission costs about three quarters of a billion dollars to remove five sizable debris from LEO. Compared to NET, ARM, and IBS, the EDT spacecraft has the highest mass since it has to carry a 250-kg EDT system throughout all maneuvers, in addition to the mass of the DEOS spacecraft. This has direct adverse effect on the removal time, required propellant mass, and total mission cost. The direct relationship between the mass of the remover spacecraft and the time required to complete the orbital maneuvers can be inferred from Eqs (1b), (2b) and (3b). Further, Eqs (9) and (10) show that the higher the mass of the spacecraft, the greater the development cost $\mathscr{D}$ and launch cost $\mathscr{L}$. As a result, the total mission cost $\mathscr{T}$ is adversely affected by the remover spacecraft mass. Also, EDT shows poor result in the performance robustness criterion, since a small variation in the orbit inclination yields to a large change in Δt_{do}. Lastly, this study focused on the removal of debris objects in highly-inclined orbits. In such orbits, the thrust generated by the EDT system is adversely affected [59]. In a nutshell, the higher the inclination, the smaller the generated drag by the EDT system.

In the performance-based approach, the IBS method also outperforms other removal methods with a utility values of 0.8298, followed by the NET method with a utility value of 0.6021. IBS mainly benefits from a low TRRA value. Using the utility function defined for the mission risk criterion and Eq. (23), it can be seen that $u > 0.5$ when $\mathscr{E}_{\text{MR}} < 53.0\%$, which is the case for LSR, NET and, IBS methods. Although in the NET method, the remover spacecraft requires to capture the target debris, it does not need as high precision as it is needed in the ARM method. The remover spacecraft in the NET method maintains a larger distance from the target debris, and as long as the net capturing mechanism is deployed in the direction of the target debris, it is highly probable that the capturing completes successfully. This is not the case in the ARM method, which requires precise capturing of the target debris from the grabbing point on the debris, thus a higher failure probability in the capturing maneuver. The shepherd spacecraft in the IBS method, the remover can also stay at a relatively far distance from the target debris so long as the ion beams fully intercept the target. LSR also benefits from staying at a far distance from the debris and hence reducing mission risks by lowering the overall expected percentage of unachieved mission objectives, $\mathscr{E}_{\text{MR}}$. The EDT method suffers from major risk factors with high consequence levels. Perhaps, the most important concern in a removal mission employing EDT method is capturing of the target debris, which requires high precision, similarly to the ARM method. Another concern would be the collision between the several kilometer-long tether and other operational and non-operational spacecraft, albeit with a low probability. The EDT method also has the highest integrated technology readiness and risk assessment (I_{TRRA}) value, due to the low TRL for the EDT module and power storage system. It should be noted that the LSR method has the highest performance robustness since the laser removal system is so powerful that the variations in the mass of target debris have minimum effect on the deorbitation time. Also, the LSR method has the lowest mission risk value, but the second largest I_{TRRA} value. Such disparity is a result of the fact that the LSR method is a contactless method, eliminating the need for rigid contact between the remover spacecraft and the target debris, which results in a low $\mathscr{E}_{\text{MR}}$. However, the laser technology and the associated power system are complex and have high AD^2 values, resulting in a high I_{TRRA} value.

In the balanced approach, NET and LSR reappear as the best performing methods and their utility scores are almost equal. This is despite the attempts to lessen the impacts of extremes from which specific removal methods may benefit or suffer, and to distribute the weights such that equal opportunities are given to all removal methods to demonstrate their capabilities. The performance of ARM and IBS methods in the balanced approach are also satisfactory.

Table 14
Normalized parameter s and unweighted utility value $u(s)$ obtained for each criterion.

Criteria	Parameter	NET	LSR	IBS	EDT	ARM
AC-1	s	0.5342	0.0000	0.5325	1.0000	0.7756
	$u(s)$	0.3745	0.9994	0.3805	0.0006	0.0158
AC-2	s	0.2805	0.0000	0.4902	1.0000	0.1068
	$u(s)$	0.9792	1.0000	0.9281	0.0000	0.9952
AC-3	s	1.0000	0.0000	0.0000	1.0000	1.0000
	$u(s)$	1.0000	0.0000	0.0000	1.0000	1.0000
AC-4	s	0.8087	0.0000	0.7217	0.9522	1.0000
	$u(s)$	0.0165	0.9820	0.0385	0.0040	0.0025
AC-5	s	0.0483	0.2828	0.1665	1.0000	0.0000
	$u(s)$	0.9712	0.7636	0.9117	0.0025	0.9820
AC-6	s	0.0000	1.0000	0.1091	0.0000	0.0000
	$u(s)$	0.9933	0.0067	0.9803	0.9933	0.9933
AC-7	s	0.2154	0.7385	0.0000	1.0000	0.2308
	$u(s)$	0.5017	0.0624	1.0000	0.0000	0.4769
AC-8	s	0.3429	0.0000	0.4857	0.5714	1.0000
	$u(s)$	0.2398	1.0000	0.1273	0.0849	0.0000

Table 15
Potential loss of each removal method based on their associated mission risks consequences and probabilities.

Method	α	C_{MR}	$\mathscr{T}$($M)	Q($M)[a]	P_{MR}	E($M)
NET	ℜ1	1		374.5	0.15	
	ℜ2	0.9	374.5	337.0	0.15	191.0
	ℜ3	0.9		337.0	0.25	
	ℜ1	0.1		47.6	0.75	
LSR	ℜ2	1	476.4	476.4	0.25	214.4
	ℜ3	0.5		238.2	0.25	
	ℜ1	0.9		383.3	0.15	
IBS	ℜ2	1	425.9	425.9	0.15	227.8
	ℜ3	0.5		212.9	0.50	
	ℜ1	1		788.2	0.15	
EDT	ℜ2	1	788.2	788.2	0.15	433.5
	ℜ3	0.5		394.1	0.50	
	ℜ1	1		353.5	0.15	
ARM	ℜ2	0.9	353.5	318.1	0.25	220.9
	ℜ3	0.5		176.7	0.50	

[a] Payoff value defined as $Q = C_{MR}\mathscr{T}$

8.3. Potential mission loss

As an additional comparison analysis, a relationship is defined, as follows, between the mission risks and total mission cost, which measures the *potential loss* (E_i) of the mission i in a worst case scenario when all risks occur given their probability and consequence level [79]:

$$E_i = \mathscr{T}_i \cdot \sum_{\alpha} C^{\alpha}_{MR,i} P^{\alpha}_{MR,i} \tag{25}$$

where $C^{\alpha}_{MR,i}$ and $P^{\alpha}_{MR,i}$ are the consequence level and the probability of occurrence of the failure mode $\alpha \in \{\Re1, \Re2, \Re3\}$ (Table 11), respectively, and $\mathscr{T}_i$ is the total mission cost (Table 9).

The results obtained from the potential loss analysis are presented in Table 15. The method with the least potential loss is NET, followed closely by LSR, ARM, and IBS. It can be seen that despite the higher *payoff* values $\mathscr{Q}$ (defined as the product of consequence level C_{MR} and the total mission cost $\mathscr{T}$) in the NET method relative to the ARM method, the NET method has a lower expected loss than ARM. This is mainly due to the fact that the failure modes considered in this study have much lower probabilities of occurrence in the NET method when compared to ARM. As stated in Section 8.2, failure mode ℜ3, i.e., the unsuccessful debris capturing, has higher probability but lower consequence in the ARM method when compared to the NET method. Further, the ARM method is more prone to the potential damages that are resulted from the uncontrolled tumbling motion of the debris. This is simply because the net capturing mechanisms are made out of elastic material (such as Dyneema [71]), which are able to compensate for and tolerate, to a certain extent, the forces exerted by the tumbling debris. In contrast, robotic manipulators are rigid bodies that can be seriously damaged in case of collisions. Arguably, the ARM method would have outperformed the NET method in the potential loss analysis if the hard and precise capturing of the debris was not required.

The IBS method in the fourth place suffers mainly from high payoff values even though the failure probabilities are relatively low. Lastly, the EDT method is adversely affected by the high mission cost (about $788) and high-precision requirements similar to ARM.

8.4. General discussions

Fig. 17 summarizes the rankings of the methods based on each assessment technique. The NET method seems to exhibit the best overall performance, followed very closely by LSR (a contactless method). ARM, exhibits a satisfactory performance across the majority of the assessment techniques, and comes in the third place. It must be noted that, despite the excellent performance of LSR, the method still suffers from not being in compliance with the IADC guidelines on controlled reentry. This may prohibit the use of laser in the removal of sizable space debris.

Considering the controlled reentry requirement, ARM and NET seem to be the most promising techniques for ADR. The methods show comparable performances in the assessment criteria (as was reflected in Fig. 14). This is mainly because of the similarities in their technologies and mission requirements. Nevertheless, nets have never been tried in space in an actual space mission. Despite the fact that several materials have been investigated for fabricating the net (such as Zylon, Dyneema, Kevlar, and Vectran [80]) a major concern regarding the net removal method is the strength of the net material. Whether the net can withstand the torsional forces after it closes around a spinning target debris is a question that is being actively investigated at the moment.

9. Conclusion

The applicability of five debris removal methods to the large LEO debris was investigated, i.e., net, laser, ion-beam shepherd,

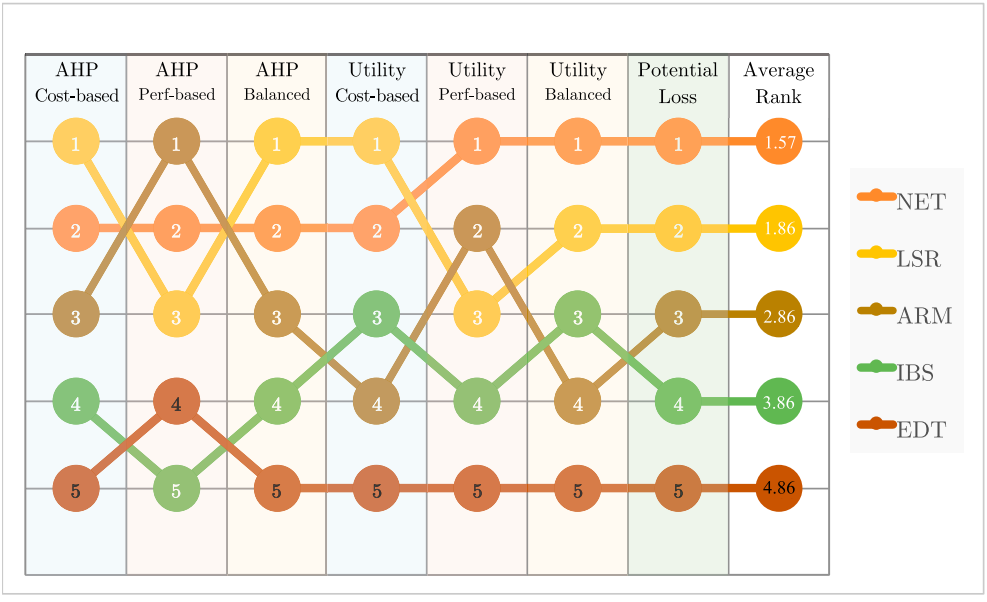

Fig. 17. Rankings of the removal methods.

electrodynamic tether, and robotic arm. A Monte Carlo simulation was used to analyze the expected performance of each removal method. The methods were compared using two assessment techniques, i.e., analytical hierarchy process and utility-based. A potential-loss analysis was also presented to highlight the effect of risks in the removal methods. The results show that net, space-based laser, and robotic arm methods appear to be more promising given the state of technologies, risks and constraints associated with the debris removal missions, and considering the uncertainty in the constituent parameters. It is worth mentioning that the study could be further extended to consider different mission scenarios for each method. For instance, it may be worth investigating an EDT-based mission concept in which the EDT modules are installed on the target debris by a chaser spacecraft, and are used independently to deorbit the debris to which they have attached. In such a case, the chaser would not need to be involved in the deorbitation, and can move on to the next target debris after installing and letting go of the composite debris-EDT system.

Further, a similar study can be conducted for the removal of shrapnel-like smaller orbital debris in LEO as well as debris removal in GEO. While the latter is essential because of the highly-valued space assets that exist in GEO, the former is becoming inevitable for the safety of astronauts in the International Space Station, and for many smaller satellites that will be operating in LEO in the future.

Appendix A. Definitions of TRL, AD^2, and TNV

Table 16
Technology readiness level according to NASA [81].

TRL	Definition	Description
TRL 1	Basic principles observed and reported.	Lowest level of TRL. Scientific research begins to be translated into applied research and development.
TRL 2	Technology concept and/or application formulated.	Invention begins, practical application is identified but is speculative, no experimental proof or detailed analysis is available to support the conjecture.
TRL 3	Analytical and experimental critical function and/or characteristic proof of concept	Analytical studies place the technology in an appropriate context and laboratory demonstrations, modeling and simulation validate analytical prediction.
TRL 4	Component and/or breadboard validation in laboratory environment	A low fidelity system/component breadboard is built and operated to demonstrate basic functionality and critical test environments, and associated performance predictions are defined relative to the final operating environment.
TRL 5	Component and/or breadboard validation in relevant environment.	A medium fidelity system/component brassboard is built and operated to demonstrate overall performance in a simulated operational environment with realistic support elements that demonstrates overall performance in critical areas. Performance predictions are made for subsequent development phases.
TRL 6	System/sub-system model or prototype demonstration in a relevant environment	A high fidelity system/component prototype that adequately addresses all critical scaling issues is built and operated in a relevant environment to demonstrate operations under critical environmental conditions.
TRL 7	System prototype demonstration in an operational environment.	A high fidelity engineering unit that adequately addresses all critical scaling issues is built and operated in a relevant environment to demonstrate performance in the actual operational environment and platform (ground, airborne, or space).
TRL 8	Actual system completed and "flight qualified" through test and demonstration.	The final product in its final configuration is successfully demonstrated through test and analysis for its intended operational environment and platform (ground, airborne, or space).
TRL 9	Actual system flight proven through successful mission operations.	The final product is successfully operated in an actual mission.

Table 17
Advancement degree of difficulty (AD^2) definition [31].

Level	Description	Risk
Level 1	Exists with no or only minor modifications being required. A single development approach is adequate.	0%
Level 2	Exists but requires major modifications. A single development approach is adequate.	10%
Level 3	Requires new development well within the experience base. A single development approach is adequate.	20%
Level 4	Requires new development but similarity to existing experience is sufficient to warrant comparison across the board. A single development approach can be taken with a high degree of confidence for success.	30%
Level 5	Requires new development but similarity to existing experience is sufficient to warrant comparison in all critical areas. Dual development approaches should be pursued to provide a high degree of confidence for success.	40%
Level 6	Requires new development but similarity to existing experience is sufficient to warrant comparison on only a subset of critical areas. Dual development approaches should be pursued in order to achieve a moderate degree of confidence for success. (desired performance can be achieved in subsequent block upgrades with high degree of confidence.	50%
Level 7	Requires new development but similarity to existing experience is sufficient to warrant comparison in only a subset of critical areas. Multiple development routes must be pursued.	70%
Level 8	Requires new development where similarity to existing experience base can be defined only in the broadest sense. Multiple development routes must be pursued.	80%
Level 9	Requires new development outside of any existing experience base. No viable approaches exist that can be pursued with any degree of confidence. Basic research in key areas needed before feasible approaches can be defined.	90-100%

Table 18
Technology need value (TNV) definition [28].

TNV	Description	W^1
TNV-01	The technology effort is **not critical at this time** to success of the program. The advances to be acheived are useful for some cost improvements; However, the information to be provided is not needed for management decisions until the far term.	40%
TNV-02	The technology effort is **useful** to the success of the program. The advances to be achieved would meaningfully improve cost and/or performance; However, the information to be provided is not needed for management decisions until the mid to far term.	60%
TNV-03	The technology effort is **important** to the success of the program. The advances to be achieved are important for performance and/or cost objectives and the information to be provided is needed for management decisions in the near to mid term.	80%

(*continued on next page*)

Table 18 (*continued*)

TNV	Description	W^1
TNV-04	The technology effort is **very important** to the success of the program. The advances to be achieved are enabling for cost goals and/or important for performance objectives and the information to be provided would be highly valuable for near term management decisions.	100%
TNV-05	The technology effort is **critically important** to the success of the program at present. The performance advances to be achieved are enabling and the information to be provided is essential for near term management decisions.	120%

[1] Weighting factor.

References

[1] NASA, Orbital Debris: Quarterly News, vol. 20, Apr. 2016 no. 1 and 2.
[2] International Telecommunication Union, Regulation of Global Broadband Satellite Communications, Apr. 2012. http://www.itu.int/ITU-D/treg/broadband/ITU-BB-Reports_RegulationBroadbandSatellite.pdf. (Accessed 23 March 2016).
[3] IADC space debris mitigation guidelines, IADC-02–01 Rev. 1, Tech. Rep, Inter-Agency Space Debris Coordination Committee, Oct. 2002.
[4] J.C. Liou, The near-earth orbital debris problem and the challenges for environment remediation, in: Proceedings of the 3rd International Space World Conference, 2012.
[5] D.J. Kessler, N.L. Johnson, J. Liou, M. Matney, The kessler syndrome: implications to future space operations, Adv. Astronaut. Sci. 137 (8) (2010) 47–61.
[6] Support to the IADC space debris mitigation guidelines, IADC-04–06, Rev 5.5, Tech. Rep, Inter-Agency Space Debris Coordination Committee, May 2014.
[7] M. Emanuelli, G. Federico, J. Loughman, D. Prasad, T. Chow, Conceptualizing an economically, legally, and politically viable active debris removal option, Acta Astronaut. 104 (1) (2014) 197–205.
[8] J.C. Liou, Active debris removal and the challenges for environment remediation, in: Proceedings of the 28th International Symposium on Space Technology and Science, 2011.
[9] J.C. Liou, Modeling the large and small orbital debris populations for environment remediation, in: Proceedings of 3rd European Workshop on Space Debris Modelling and Environment Remediation, 2014.
[10] H. Lewis, A. White, R. Crowther, H. Stokes, Synergy of debris mitigation and removal, in: International Astronautical Congress, 2011. IAC-11–A6.4.5.
[11] J.C. Liou, A. Anilkumar, B.B. Virgili, T. Hanada, H. Krag, H. Lewis, M.X.J. Raj, M.M. Rao, A. Rossi, R.K. Sharma, Stability of the future LEO environment: an iadc comparison study, in: Proceedings of the 6th European Conference on Space Debris, 2013. At Darmstadt, Germany.
[12] T. Kelso, NORAD two-line element sets: current data, https://celestrak.com/NORAD/elements/, accessed: 2017-10-01.
[13] V. Braun, A. Lupken, S.K. Flegel, J. Gelhaus, M. Moeckel, C. Kebschull, C. Wiedermann, P. Vorsmann, Active debris removal of multiple priority targets, Adv. Space Res. 51 (9) (2013) 1638–1648.
[14] B.B. Virgili, H. Krag, Strategies for active removal in LEO, in: Proceedings of the 5th European Conference on Space Debris, 2009.
[15] L. Jasper, P. Anderson, H. Schaub, D.S. McKnight, Economic and risk challenges of operating in the current space debris environment, in: Proceedings of the 3rd European Workshop on Space Debris Modeling and Remediation, 2014.
[16] P. Chrystal, D. McKnight, P. Meredith, Space Debris: on Collision Course for Insurers?, Tech. Rep, Swiss Insurance Company Ltd, 2011.
[17] United Launch Alliance, Atlas V Lanuch Services: User's Guide, 2010.
[18] M.C. Bazzocchi, M.R. Emami, Comparative analysis of redirection methods for asteroid resource exploitation, Acta Astronaut. 120 (2016) 1–19. https://doi.org/10.1016/j.actaastro.2015.11.021.
[19] T. Kelso, SATCAT operational status, https://celestrak.com/satcat/status.asp, accessed: 2017-07-12.
[20] ESA, Database and information system characterising objects in space (DISCOS), https://discosweb.esoc.esa.int/web/guest/home;jsessionid=a4366be522ba6d20ab13dd31ea0e, accessed: 2016-02-23.
[21] A. Ruggiero, P. Pergola, S. Marcuccio, M. Andrenucci, Low-thrust maneuvers for the efficient correction of orbital elements, in: Proceedings of the 32nd International Electric Propulsion Conference, 2011.
[22] Massachusetts Institute of Technology, Analytical approximations for low thrust maneuvers, https://ocw.mit.edu/courses/aeronautics-and-astronautics/16-522-space-propulsion-spring-2015/lecture-notes/MIT16_522S15_Lecture6.pdf, accessed: 2017-07-14.
[23] F. Aghili, Time-optimal detumbling control of spacecraft, J. Guid. Contr. Dynam. 32 (5) (2009) 1671–1675. https://doi.org/10.2514/1.43189.
[24] ESA Space Debris Mitigation WG, ESA Space Debris Mitigation Compliance Verification Guidelines, ESSB-HB-u-002, 2015.
[25] NASA Cost Estimating Handbook, Version 4.0, 2015. https://www.nasa.gov/sites/default/files/files/01_CEH_Main_Body_02_27_15.pdf. (Accessed 23 March 2016).
[26] J.R. Wertz, D.F. Everett, J.J. Puschell, Space Mission Engineering: the New SMAD, Microcosm Press, Howthorne, CA, 2011.
[27] Gunter's Space, Atlas-5, http://space.skyrocket.de/doc_lau/atlas-5.htm, accessed: 2016-03-08.
[28] J.C. Mankins, Technology readiness and risk assessments: a new approach, Acta Astronaut. 65 (2009) 1208–1215. https://doi.org/10.1016/j.actaastro.2009.03.059.
[29] J.C. Mankins, The Case for Space Solar Power, Virginia Edition Publishing, LLC, Houston USA, 2014.
[30] NASA, Technology readiness level, https://www.nasa.gov/directorates/heo/scan/engineering/technology/txt_accordion1.html, accessed: 2016-03-08.
[31] M. Macdonald, V. Badescu, The International Handbook of Space Technology, Springer, 2014.
[32] Goddard Space Flight Center, Risk Management Reporting GSFC-STD-0002, 2009. https://www.nasa.gov/directorates/heo/scan/engineering/technology/txt_accordion1.html. (Accessed 8 March 2016).
[33] NASA, Risk Management Reporting, Tech. Rep. GSFC-STD-0002, National Aeronautics and Space Administration (NASA), Goddard Space Flight Center, 2009.
[34] Airbus Defence and Space, Electric Propulsion Thruster Family, 2013.
[35] C. Bombardelli, M. Merino-Martínez, E.A. Galilea, J. Peláez, H. Urrutxua, J. Herrera-Montojo, A. Iturri-Torrea, Ariadna Call for Ideas: Active Removal of Space Debris, Ion Beam Shepherd for Contactless Debris Removal, Jul. 2011. Final Rep. 4000101447/10/NL/CBi.
[36] H.J. Leiter, R. Killinger, H. Bassner, J. Müller, R. Kukies, Development of the Radio Frequency Ion Thruster RIT XT Â€“ a Status Report, Tech. Rep, Astrium GmbH, 2001.
[37] M. Loesch, F. de Bruin, M. Castronuovo, F. Covello, J. Geary, S. Hyde, W. Jung, F. Longo, M.M. Fernandez, S. Mason, K. Springborn, S. Wagenbach, J. Kreisel, Economic approach for active space debris removal services, in: Proceedings of the 10th International Symposium on Artificial Intelligence, Robotics and Automation in Space (i-SAIRAS) 2010, 2010.
[38] K. Wormnes, R. Le Letty, L. Summerer, ESA technologies for space debris remediation, in: Proceedings of the 6th Conference on Space Debris, ESA/ESTEC, 2013.
[39] ESA, How to Catch a Satellite?, 2014. http://www.esa.int/Our_Activities/Space_Engineering_Technology/Clean_Space/How_to_catch_a_satellite. (Accessed 23 February 2016).
[40] ESA, Robotic Geostationary Orbit Restorer (ROGER), 2014. http://www.esa.int/Our_Activities/Space_Engineering_Technology/Automation_and_Robotics/RObotic_GEostationary_orbit_Restorer_ROGER. (Accessed 23 March 2016).
[41] S. Bondarenko, S. Lyagushin, G. Shifrin, Prospects of using lasers and military space technology for space debris removal, in: Proceedings of the 2nd European Conference on Space Debris, 1997.
[42] T.D. Bell, Weaponization of Space: Understanding Strategic and Technical Inevitabilities (Occasional Paper No. 6), 1999. http://www.au.af.mil/au/awc/awcgate/cst/csat6.pdf. (Accessed 30 March 2016).
[43] C.R. Phipps, T.P. Turner, R.F. Harrison, G.W. York, W.Z. Osborne, G.K. Anderson, X.F. Corlis, L.C. Haynes, H.S. Steele, K.C. Spicochi, T.R. King, Impulse coupling to targets in vacuum by KrF, HF, and CO^2 singleâ€pulse lasers, J. Appl. Phys. 64 (3) (1988) 1083–1096. https://doi.org/10.1063/1.341867.
[44] C.R. Phipps, L'ADROIT - a spaceborne ultraviolet laser system for space debris clearing, Acta Astronaut. 104 (1) (2014) 243–255, https://doi.org/10.1016/j.actaastro.2014.08.007.
[45] S.H. Choi, R.S. Papa, Assessment study of small space debris removal by laser satellites, Recent Pat. Space Technol. 5 (2) (2015) 116–122.
[46] A. Gibbings, M. Vasile, J.-M. Hopkins, D. Burns, I. Watson, Experimental characterization of the thrust induced by laser ablation onto an asteroid, in: IAA Planetary Defense Conference, 2012.
[47] R. Soulard, M.N. Quinn, T. Tajima, G. Mourou, ICAN: a novel laser architecture for space debris removal, Acta Astronaut. 105 (1) (2014) 192–200. https://doi.org/10.1016/j.actaastro.2014.09.004.
[48] S. Shen, X. Jin, C. Hao, Cleaning space debris with a space-based laser system, Chin. J. Aeronaut. 27 (4) (2014) 805–811. https://doi.org/10.1016/j.cja.2014.05.002.
[49] M. Kaplan, Survey of space debris reduction methods, in: AIAA SPACE 2009 Conference & Exposition, American Institute of Aeronautics and Astronautics, 2009, https://doi.org/10.2514/6.2009-6619.
[50] J.-C. Liou, Engineering and Technology Challenges for Active Debris Removal, 2013, https://doi.org/10.1051/eucass/201304735.
[51] S. Kitamura, Large space debris reorbiter using ion beam irradiation, in: Proceedings of the 61st International Astronautical Congress (IAC 2010), 2010.
[52] C. Bombardelli, J. Peláez, Ion beam shepherd for contactless space debris removal, J. Guid. Contr. Dynam. 34 (3) (2011) 916–920, https://doi.org/10.2514/1.51832.
[53] C. Bombardelli, H. Urrutxua, M. Merino, E. Ahedo, J. Pelaez, J. Olympio, Dynamics of ion-beam propelled space debris, in: Proceedings of the 22nd Symposium on Space Flight Dynamics, 2011.
[54] R.P. Hoyt, Propulsion and power harvesting performance of electrodynamic tether, in: AIAA SPACE 2011 Conference and Exposition, 2011, https://doi.org/10.2514/6.2011-7321.
[55] R. Forward, R. Hoyt, Application of the Terminator Tether™ electrodynamic drag technology to the deorbit of constellation spacecraft, in: Proceedings of the 34th AIAA/ASME/SAE/ASEE Joint Propulsion Conference and Exhibit, American Institute of Aeronautics and Astronautics, 1999.

[56] M. Macdonald, C. McInnes, C. Bewick, L. Visagie, V. Lappas, S. Erb, Concept-of-operations disposal analysis of spacecraft by gossamer structure, J. Spacecraft Rockets 52 (2) (2015) 517–525.
[57] R. Hoyt, R. Forward, Performance of the Terminator Tether™ for autonomous deorit of leo spacecraft, in: Proceedings of the 35th AIAA/ASME/SAE/ASEE Joint Propulsion Conference and Exhibit, American Institute of Aeronautics and Astronautics, 1999.
[58] STI SpaceTech GmbH, DEOS phase a datasheet, http://www.spacetech-i.com/images/press/downloads/DEOS_PhaseA_Datasheet.pdf, accessed: 2016-03-23.
[59] C. Pardini, T. Hanada, P.H. Krisko, Potential benefits and risks of using electrodynamic tethers for end-of-life de-orbit of LEO spacecraft, Tech. rep, Inter-Agency Space Debris Coordination Committee (IADC), 2006.
[60] R.P. Patera, Method for calculating collision probability between a satellite and a space tether, J. Guid. Contr. Dynam. 25 (5) (2002) 940–945. https://doi.org/10.2514/2.4967.
[61] M. Nohmi, Initial orbital performance result of nano-satellite stars-ii, in: Proceedings of the International Symposium on Artificial Intelligence, Robotics and Automation in Space (I-SAIRAS), 2014.
[62] G. Hirzinger, K. Landzettel, B. Brunner, M. Fischer, C. Preusche, D. Reintsema, A. Albu-Schäffer, G. Schreiber, B.-M. Steinmetz, DLR's robotics technologies for on-orbit servicing, Adv. Robot. 18 (2) (2004) 139–174. https://doi.org/10.1163/156855304322758006.
[63] A. Flores-Abad, A review of space robotics technologies for on-orbit servicing, Prog. Aero. Sci. 68 (2014) 1–26. https://doi.org/10.1016/j.paerosci.2014.03.002.
[64] T. Wolf, DEOS: the in-flight technology demonstration of German's robotics approach to dispose malfunctioned satellites, in: Proceedings of the 11th Symposium on Advanced Space Technologies in Robotics and Automations (ASTRA 2011), 2011.
[65] P. Colmenarejo, M. Avilés, E. di Sotto, Active debris removal GNC challenges over design and required ground validation, CEAS Space Journal 7 (2) (2015) 187–201, https://doi.org/10.1007/s12567-015-0088-y.
[66] M. Macdonald, C. McInnes, C. Lücking, L. Visagie, V.J. Lappas, S. Erb, Needs assessment of gossamer structures in communications platform end-of-life disposal, in: AIAA Guidance, Navigation, and Control (GNC) Conference, American Institute of Aeronautics and Astronautics, 2013, https://doi.org/10.2514/6.2013-4870.
[67] ESA, RemoveDebris Mission, 2016. https://directory.eoportal.org/web/eoportal/satellite-missions/r/removedebris. (Accessed 24 March 2016).
[68] J. Sanchez, C. Colombo, M. Vasile, G. Radice, Multicriteria comparison among several mitigation strategies for dangerous near-earth objects, J. Guid. Contr. Dynam. 32 (1) (2009) 121–142, https://doi.org/10.2514/1.36774.
[69] D. Smitherman, A comparison of a solar power satellite concept to a concentrating solar power system, in: Proceedings of AIAA SPACE 2013 Conference and Exposition, American Institute of Aeronautics and Astronautics, 2013.
[70] Steering Committee for NASA Technology Roadmaps, NASA space technology roadmaps and priorities: Restoring NASA's technological edge and paving the way for a new era in space, The National Academic Press, Washington, DC, 2012.
[71] A. Medina, L. Cercos, R. Stefanescu, R. Benvenuto, M. Lavagna, I. Gonzalez, N. Rodriguez, K. Wormnes, Capturing nets for active debris removal: a follow-up microgravity experiment design to validate flexible dynamic models, in: 13th Symposium on Advanced Space Technologies in Robotics and Automation, ESA/ESTEC, 2015.
[72] S. Shuangyan, J. Xing, C. Hao, Cleaning space debris with a space-based laser system, Chin. J. Aeronaut. 27(4).
[73] J. Melman, E. Mooij, R. Noomen, State propagation in an uncertain asteroid gravity field, Acta Astronaut. 91 (2013) 8–19. https://doi.org/10.1016/j.actaastro.2013.04.027.
[74] V. Chobotov, D. Mains, Tether satellite system collision study, Acta Astronaut. 44 (7) (1999) 543–551. https://doi.org/10.1016/S0094-5765(99)00098-3.
[75] D. Zanutto, Analysis of propellantless tethered system for the de-orbiting of satellites at end of life, Ph.D. thesis, Università degli Studi di Padova, 2013.
[76] J.R. Wertz, R. Bell, Autonomous rendezvous and docking technologies–status and prospects, in: Space Systems Technology and Operations Conference, 2003.
[77] R. Biesbroek, ESA's e.deorbit mission and its roadmap to active debris removal, in: Proceedings of the 5th CEAS Air and Space Conference, 2015.
[78] T.L. Saaty, Decision making with the analytic hierarchy process, Int. J. Serv. Sci. 1 (1) (2008) 83–98.
[79] B. Hyman, Fundamentals of Engineering Design, second ed., Pearson Education Ltd, 2002.
[80] R. Benvenuto, R. Carta, Active debris removal system based on tethered-nets: experimental results, in: Proceedings of the 9th Pegasus-AIAA Student Conference, American Institute of Aeronautics and Astronautics, 2013.
[81] NASA, Technology readiness level definitions, http://www.nasa.gov/pdf/458490main_TRL_Definitions.pdf, accessed: 2016-03-03.